

Final Degree Project



Understanding metabolic and stress changes in mitochondrial disease. A case study in Leber's Hereditary Optic Neuropathy.

Report Type D: Experimental + Investigation Project

Centro de Investigaciones Biológicas 'Margarita Salas' - CSIC
Universidad Francisco de Vitoria

Student: Ignacio Monar Redondo
Advisor: Dr. Aurora Gómez-Durán
Internal mentor: Dr. Teresa de Asua

Madrid, 10th September 2020

Index

Index	1
Abstract	2
Introduction. Bibliographic revision.	3
I. Mitochondria and OXPHOS	3
II. Mitochondrial genome	4
III. Mitochondrial diseases (MDs)	5
A. Point mutations in the mtDNA	6
B. Mutations affecting mitochondrial translation	7
C. Major rearrangements of the mtDNA	8
IV. Metabolic changes in MDs	8
A. Conventional biomarkers	8
B. Novel biomarkers	12
V. Mitochondrial dysfunction and stress mechanisms	16
A. mTORC1	17
B. Integrated stress response (ISR)	17
C. Role ATF4 in MDs	19
Methods	20
I. Bibliographic research	20
II. Cell culturing	21
III. Denaturing electrophoresis and Western blot analysis.	22
IV. Real-time PCR quantification of transcripts.	23
V. Statistical analysis and graphics	24
Results	25
Case-study: Unmasking the mechanisms of stress in cell lines with mutations causing LHON.	25
A. eIF2A is activated in m.3460G>A	25
B. mTORC1 is activated in m.11778G>A	27
C. No differences are observed in PERK levels	28
D. mtUPR is not activated in LHON cell lines	29
E. ATF4 is transcriptionally downregulated in m.3460G>A cell line	30
F. ER stress is not activated in cell lines carrying LHON mutations	31
Discussion and conclusions	33
Bibliography	35
Acknowledgements	45

Abstract

Mitochondria are organelles which perform various roles in the cell (mainly the energy production) and house their own genetic material, the mitochondrial DNA. Mutations in this genome and/or genes of the nuclear DNA affecting mitochondrial function are the cause of a set of rare pathologies (1 patient:5000 individuals) known as mitochondrial diseases (MDs). MDs comprise a wide range of disorders with high phenotypic variability and unknown molecular mechanisms, which limits their diagnosis and treatment. Recently, multi-omic approaches have emerged as a possible tool to identify new biomarkers and pathways involved in these pathologies pointing to fundamental metabolic routes such as the mechanistic target of rapamycin complex 1, the Integrated Stress Response and the Activating Transcription Factor 4. Here, we present a comprehensive review of the latest insights in the field, compiling recent publications on metabolomics as well as transcriptomic data trying to dissect the puzzle underlying the complexity MDs. In addition, we perform a case study on cell lines carrying two primary mutations causing Leber's Hereditary Optic Neuropathy to investigate how different elements of cellular stress are altered in this disease. Interestingly, we find a mutation-specific response which might be related to the severity of the variant.

Introduction. Bibliographic revision.

I. Mitochondria and OXPHOS

Mitochondria are very complex and dynamic organelles constantly fusing and budding¹ which synthesize the most of the energy of the cell in the form of adenosine triphosphate (ATP). Mitochondria are not only the powerhouse of the cell but also integrate multiple metabolic pathways, such as fatty acid oxidation, urea cycle, gluconeogenesis and ketogenesis. Furthermore, they play an important role in other cellular processes like non-shivering thermogenesis, amino acid metabolism, lipid metabolism, biosynthesis of haem and iron-sulfur clusters, calcium homeostasis and apoptosis².

Cells are able to produce reducing equivalents nicotinamide adenine dinucleotide (NAD(P)H) and flavin adenine dinucleotide (FADH₂) by various metabolic routes. These molecules are reoxidized in the mitochondria in order to be recovered and cease their electrons to the electron transport chain (ETC). This process, together with the synthesis of ATP, is known as oxidative phosphorylation (OXPHOS). OXPHOS's reactions take place in the inner membrane, which is heavily folded in order to increase its surface and achieve a higher activity. OXPHOS is formed by five complexes (named I - V) and two mobile electrons carriers (CoQ/ubiquinone and cytochrome C). All the elements of the ETC are arranged (Fig. 1) in increasing order of potential of reduction, so that the electrons flow spontaneously following the thermodynamic rules. This makes it possible to generate energy through some endergonic reactions, which is accumulated as a gradient of protons (H⁺). Then, the complex V - ATP synthase is able to leverage this energy transforming it into ATP molecules and restoring the H⁺ balance³.

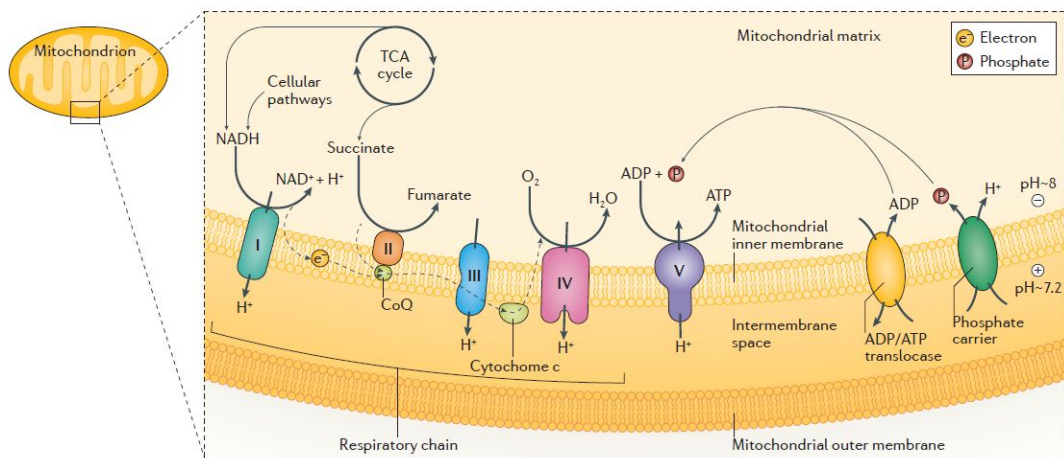


Fig. 1: Schematic representation of oxidative phosphorylation. Taken from Gorman et al. (2016)². Complex I (NADH:coenzyme Q oxidoreductase); coenzyme Q10 (CoQ); complex II (succinate-CoQ oxidoreductase); complex III (ubiquinol-cytochrome c oxidoreductase); complex IV (cytochrome c oxidase); complex V (ATP synthase).

II. Mitochondrial genome

Mitochondria house their own genome, codified in a circular molecule of double stranded DNA known as mitochondrial DNA (mtDNA). In mammals, it is maternally inherited and does not present recombination⁴. During fecundation, one of the few spermatozoa that reach the corona radiata destroys the zona pellucida by releasing digestive enzymes (contained in the acrosomes) and fuses with the oocyte membrane. Then, only the nuclear genetic material of the male is released onto the egg cytoplasm allowing pronucleus fusion and formation of the zygote. Thus, the only mtDNA inherited comes from the ovocyte⁵.

The mtDNA molecule lacks histones and has a high density of coding sequences, similar to prokaryotic DNA⁶. It is 16,569 base pairs long and polyploid, being present in several copies in each single mitochondria, and thus per cell. This fact leads to the situation of heteroplasmy. Heteroplasmy happens when in a single mitochondrion/cell there are mtDNA molecules with alternative alleles in their sequence, providing a pool of mitochondrial genomes. Likewise, different cells might hold distinct heteroplasmy levels and variants, resulting in an unique distribution of alterations in each tissue, organ and individual which eventually undergo the particular consequences of these variations⁷.

mtDNA encodes for 13 polypeptides of the oxidative phosphorylation system (OXPHOS), along with 22 transfer RNAs (tRNAs) and 2 ribosomal RNAs (rRNAs) necessary for the transcription and translation inside the mitochondria (Fig. 2). The remaining proteins involved in mitochondrial function (more than 1,500)⁸ are encoded in the nuclear DNA (nDNA), synthesized in the cytosol and imported into the mitochondria⁹. These proteins include enzymes of mitochondrial metabolic routes, components of the ETC and assembly factors, chaperones, nucleases, carriers, ribosomal proteins, etc⁸.

III. Mitochondrial diseases (MDs)

Genetic variants in the genomes encoding for proteins involved in the mitochondrial function (mtDNA and/or nDNA) cause rare diseases known as mitochondrial diseases (MDs)². These disorders are normally characterised by changes in mitochondrial function, affecting the bioenergetics and/or the metabolic network of the cell. MDs present a wide range of phenotypes with a multi-organic involvement¹⁰ and a complex etiology, as one single mutation can result in several types of syndromes, or the opposite. For example, the m.3243A>G mutation in *MT-TL1* might cause chronic progressive external ophthalmoplegia (CPEO), lactic acidosis and stroke-like episodes syndrome (MELAS) and maternally inherited diabetes and deafness (MIDD)⁵. Nowadays, little is known about how these mutations affect different tissues and organs with such variable degree of severity⁷. Further knowledge on the molecular basis of these pathologies will benefit their diagnosis and discovery of effective therapies.

Alterations in the mtDNA account for the majority of MDs in adults, while in children they are less common as phenotypic manifestation requires a high level of heteroplasmy². Point mutations in the mtDNA can either affect protein-encoding genes or disturb the protein synthesis inside the organelle, altering *mt-tRNA* and/or *mt-rRNA* genes¹¹. We have selected some of the most studied MDs caused by point mutations and rearrangements in the mtDNA (representing most of the MDs patients) and classified them in whether they cause a point mutation in a gene encoding any of the OXPHOS complexes, a defect in the mitochondrial translation and/or mtDNA level changes.

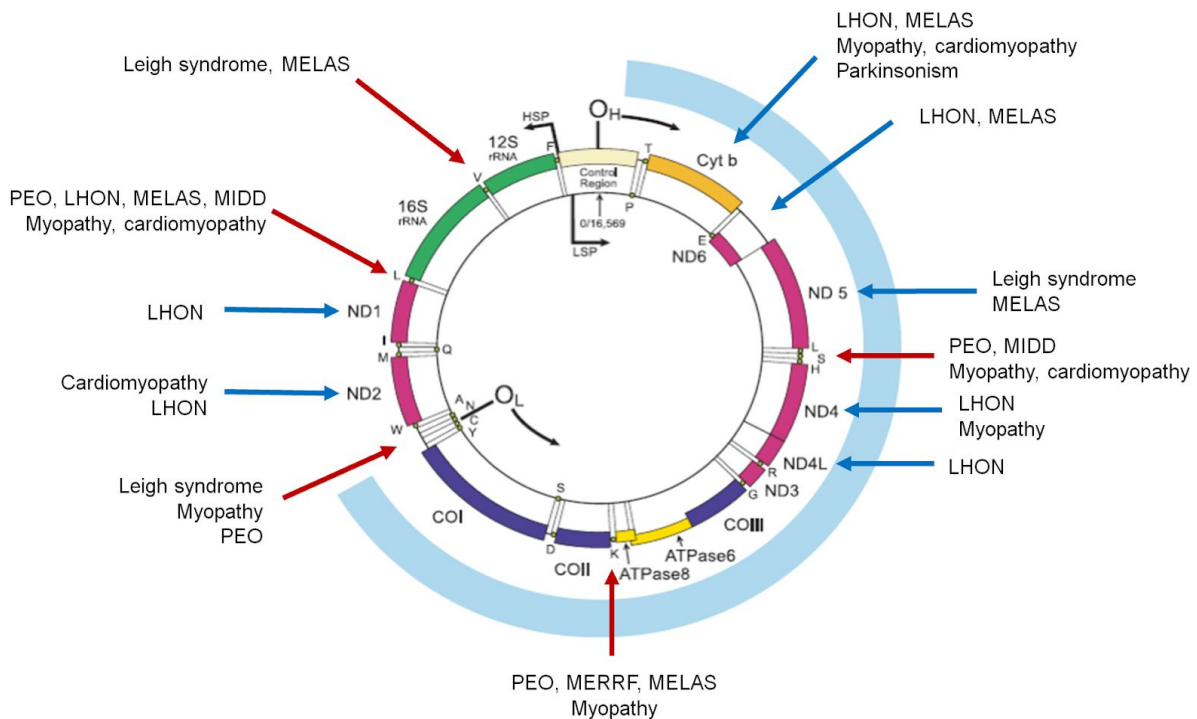


Fig. 2: The mitochondrial genome and map of mutations causing mitochondrial disorders in the mtDNA. Adapted from *Biochemistry* (C. Mathews)³. Colours pink, orange, blue and yellow show genes encoding for complex I, III, IV and V subunits, respectively. Green is used for genes encoding for rRNAs and black lines for tRNAs. Red and blue arrows highlight variants affecting mitochondrial translation and point mutations in OXPHOS complexes, respectively.

A. Point mutations in the mtDNA

Point mutations in the genes encoding for subunits of OXPHOS complexes cause a variety of disorders. One example for this type of disorders is the Leber's Hereditary Optic Neuropathy (LHON), caused by missense mutations in the mtDNA that can act individually or in association with others. The three commonest mutations causing LHON are the non-synonym changes m.3460G>A/p.MT-ND1:A52T, m.11778G>A/ p.MT-ND4:R340H and m.14484T>C/ p.MT-ND6:M64V. These alterations affect polypeptides from complex I¹². It is maternally inherited as it arises from a mtDNA alteration, affecting mostly young males¹³. LHON patients present acute or subacute central vision loss leading to scotoma or deafness. Alterations rising from these mutations affect selectively retinal ganglion cells (RGCs) functionality, but some cases can present cardiac and neurological abnormalities. Incomplete penetrance and gender bias seem to rely on genetic and environmental factors¹⁴.

Another well studied MD caused by point mutations in a wide range of genes in either nDNA or mtDNA is Leigh syndrome (LS)¹⁵. LS is a dramatic neurodegenerative disorder characterized by early deaths in childhood or young adulthood, normally not older than 3 years. The most common genetic causes are defects in complex I, but reported cases involving other complexes, assembly factors, mtDNA maintenance and mitochondrial translation machinery have also been described¹⁶.

A sub-type of LS is caused by mutations in the *MT-ATP6* gene, which encodes for subunit 6 of complex V (CV) and is known as Maternally inherited LS (MILS). However, strikingly the same mutations that cause MILS provoke Neuropathy, Ataxia and Retinitis Pigmentosa (NARP) depending on the heteroplasmy degree (mtDNA mutant content)¹⁷. When the levels of heteroplasmy are >80% causes LS (MILS) and is characterized by onset of symptoms typically between ages three and 12 months, with very bad prognosis as described above. But, when the heteroplasmic load is <80% causes NARP syndrome that can be relatively stable for many years and with a less acute phenotype. In both cases, the pathogenesis is thought to be caused by ATP synthesis impairment¹⁸. But other genetic factors such as the mtDNA background (collection of population variants on the mtDNA) might play a key role as it can derive in respiratory chain (RC) defects that contribute to phenotypic variability¹⁹.

B. Mutations affecting mitochondrial translation

MELAS syndrome can be caused by mutations in several mt-tRNA genes, but the most common is the m.3243A>G conversion in the *MT-TL1* gene²⁰. Rarely it can be caused by mutations in complexes I, III or IV. The clinical phenotype is variable and it includes neurological, muscular, cardiac and gastrointestinal manifestations and lactic acidemia²¹. Importantly, high heteroplasmy levels of m.3243A>G mutation affect neuronal network organization and activity²², which could stand for cognitive and psychiatric characteristics of MELAS.

Highlighting the complexity of MDs, MIDD shares with MELAS the m.3243A>G mutation as the most common cause of the disease. Mutations in other mt-tRNA genes have also been related to MIDD²³. It is characterized by hearing loss and diabetes, but patients can present symptoms related to other MDs²⁴.

Interestingly, patients harbouring the m.3243A>G mutation present a wide spectrum of phenotypic manifestations, ranging from MIDD to MELAS. It is commonly accepted that higher heteroplasmy levels lead to more severe affectations, but other factors such as mtDNA copy number²⁵, environmental factors²⁶ or nuclear genetic factors²⁷ might also be determining in the final phenotype. Further investigation will hopefully allow us to identify these factors and unravel the pathophysiological mechanisms which participate in these and other mitochondrial disorders.

C. Major rearrangements of the mtDNA

Infantile Onset Spinocerebellar Ataxia (IOSCA) is caused by multiple deletions in the mtDNA mainly in skeletal muscle, derived from mutations in the nDNA encoded Twinkle helicase which disturbs mtDNA replication. Symptoms include difficulty to coordinate movements (ataxia), muscle weakness (hypotonia), involuntary writhing of the limbs (athetosis) and other neurodegenerative manifestations. It is autosomal recessively inherited and appears in children from 9-18 months²⁸.

Progressive external ophthalmoplegia (PEO) is a mitochondrial myopathy driven by mutations in the nDNA-encoded DNA polymerase gamma gene (*POLG*), which derives in multiple deletions in the mtDNA. It is characterized by weakness of the external eye muscles²⁹.

IV. Metabolic changes in MDs

Mitochondria produce the majority of energy in the cell, but they are also an intersection point between multiple metabolic routes³⁰. Thus, variants causing MDs also compromise several intra-mitochondrial OXPHOS catabolism that affect the function of other cytoplasmic signals and metabolites. Finding the ins and outs of these metabolic imbalance is crucial for diagnosis (disease biomarkers) and therapeutics of these disorders.

A. Conventional biomarkers

Several metabolic biomarkers have been traditionally used in diagnosis of MDs. Some of them include lactate, pyruvate, creatine kinase and alanine (see Table 1).

A classical biomarker in MDs is lactic acid or lactate (Table 1). Cells respond to the mitochondrial dysfunction performing homolactic fermentation. Under OXPHOS deficiency, the pyruvate originated from the glycolysis is stalled, accumulates and its transformed by the lactate dehydrogenase (LDH) into lactate (Fig. 3), that is then released to the body fluids, such as the blood and cerebrospinal fluid (CSF) causing lactic acidosis. The ratio of lactate:pyruvate is commonly employed as a biomarker in several MDs. However, their use is debatable, as many disorders such as Kearns-Sayre syndrome, LHON, and mitochondrial polymerase γ -associated patients do not show high lactate³¹. In addition, the measurement and analysis of lactate is complex and limited which makes its reliability uncertain^{32,33}. Similarly, the pyruvate is also very unstable^{34,35} and is often misestimated³¹. Besides, its increase can be a confounder of other metabolic diseases such as the pyruvate dehydrogenase (PDH) deficiency³⁶. All together, these facts make them non-reliable, encouraging the discovery of new biomarkers.

Several MDs show increased alanine levels³³ (Table 1). Alanine is produced from pyruvate and glutamate by the enzyme alanine transaminase (ALT) along with α -ketoglutarate (α -KG) (Fig. 3). Normally, an increase in the levels of alanine is a reflection of pyruvate accumulation³³. Thus, it has been proposed as a viable biomarker when considered along with other metabolites³⁷. Alanine measurement is also easier than lactate and pyruvate as it has higher stability during collection of the sample³³. High levels of alanine have been observed in patients with IOSCA, MIRAS, PEO and MELAS/MIDD (see Table 1). Alterations in the levels of alanine are not exclusive to MDs but present in PDH and pyruvate carboxylase (PC) deficiency³³, as well as other pathologies such as thiamine deficiency³⁸.

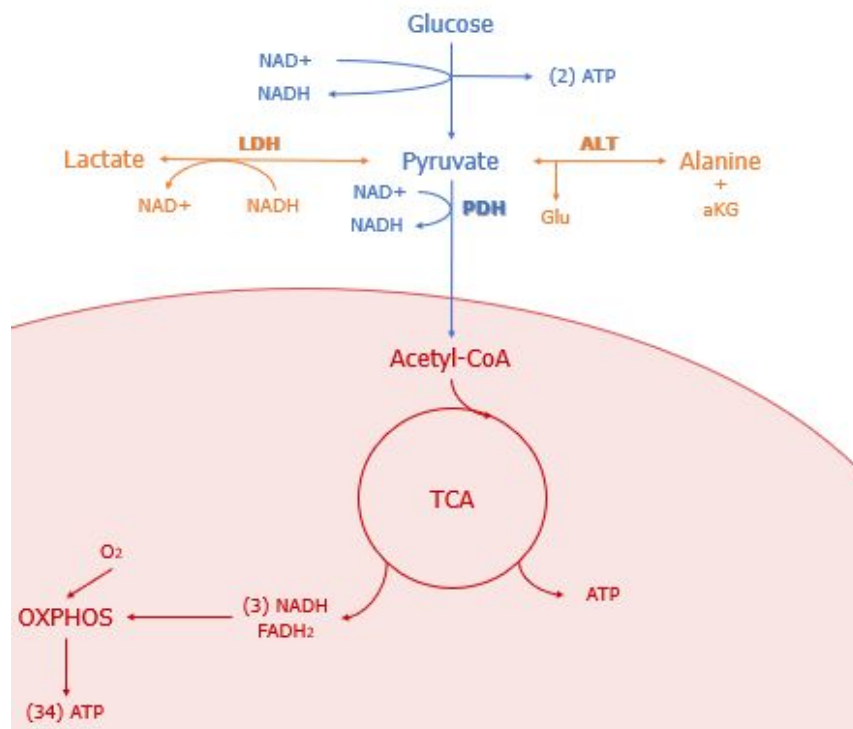


Fig. 3: Scheme of the main sources of pyruvate production in the cell. TCA: tricarboxylic acid cycle; aKG: alpha ketoglutarate; Glu: glutamate; LDH: lactate dehydrogenase; ALT: alanine transaminase; PDH: pyruvate dehydrogenase; NADH: nicotinamide adenine dinucleotide; FADH₂: flavin adenine dinucleotide; ATP: adenosine triphosphate.

The third classical biomarker in MDs is creatine (Cr). Creatine acts as storage or transport of high-energy phosphate groups ensuring ATP/adenosine diphosphate (ADP) buffering³⁹ that allows the transfer of one phosphate group from ATP to yield phosphocreatine (PCr) and ADP through the creatine kinase (CK) reaction (Fig. 4). Under OXPHOS deficiency, and thus ATP depletion, the Cr accumulates by shifting the CK reaction into Cr production (Fig. 4). High Cr plasma levels have been reported in LS⁴⁰, IOSCA³⁷, MELAS and MERRF⁴¹ (see Table 1). However, Cr in blood can be also affected by factors such as diet, exercise, age and gender⁴¹ limiting its use as a reliable marker for MDs.

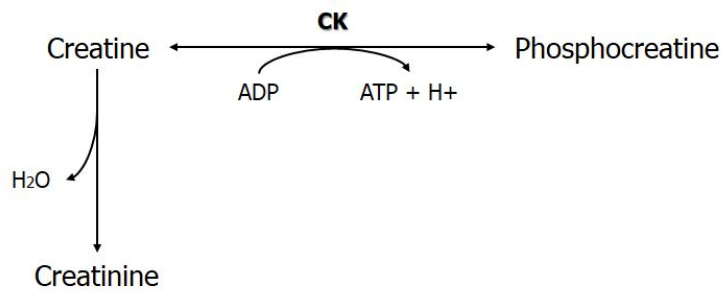


Fig. 4: The creatine kinase (CK) reaction and the non-enzymatic production of creatinine.

Carnitine has also been suggested as a potential MD biomarker as it is related to fatty acid oxidation. Low acylcarnitines C3 and C5 levels have been reported in LHON fibroblasts⁴², and altered levels of other acylcarnitines (Table 1) have been found in LS patients⁴⁰. Alterations in blood and urine concentrations of other organic acids - highlighting TCA cycle intermediates - also occur in MDs^{33,41,43,44}. However, these findings do not provide a clear metabolic pattern in MDs and further investigation is needed.

Similar to the described biomarkers, other molecules have been reported in isolated disorders. Some examples are the nitric oxide (NO) and arginine deficiency which are strikingly related to the pathogenesis of MELAS patients⁴⁵. High levels of thymidine and deoxyuridine are characteristic of mitochondrial neurogastrointestinal encephalopathy (MNGIE)⁴⁶ and serve as good biomarkers of this particular disease.

METABOLITE	ALTERATION	ASSOCIATED DISEASE/MUTATION	PUBLISHED ON
lactate	increase	OXPHOS disorders	Smeitink 2006
	increase	Leigh syndrome	Rahman 2001
	increase	Leigh syndrome	Ugalde 2003
	increase	Leigh syndrome	Lake 2016
	increase	LSCF	Olahova 2015
	increase	IOSCA	Sarzi 2007
	increase	A354V o C1277STOP en LRPPRC (assembly of CIV) - LSFC	Thompson-Legault 2015
	increase	heteroplasmic T8993G mtDNA mutation (mT80) - NARP/MILS syndrome	Gaude 2018
	increase	MELAS	Chung 2020
	increased secretion	pipecidin+oligomycin treatment	To 2019
	increased secretion	rotenone and actimycin treatment	Shaham 2009
	increased plasma levels	various MDs (MELAS, MERRF, mtDNA depletion and deletions)	Shaham 2009
	increased plasma levels	various MDs	Clarke 2013
	increased plasma levels	MNGIE	Filosto 2018
	increased CSF levels	MELAS	El-Hattab2015
	increased CSF levels	MELAS	Koga 2011
	increased CSF levels	CoQ10 deficiency syndrome (Cox9 R239X/R239X mouse)	Barriocanal-Casado 2019
	increased urine levels	various MDs	Alban 2017
alanine	increased plasma, urine and CSF levels	MILS	Thorburn 2017
	remains stable	LHON	Morvan 2018
	increase	A354V o C1277STOP en LRPPRC (assembly of CIV) - LSFC	Thompson-Legault 2015
	increase	homoplasmic T8993G mtDNA mutation in A6MT - NARP/MILS syndrome	Chen 2018
	increase	MIRAS	Buzkova 2018
	increase	MELAS/MIDD	Buzkova 2018
	increase	OXPHOS disorders	Smeitink 2006
	increase	A3243G mutated cells	Chung 2020
	increased plasma levels	Deletor mouse	Tyynismaa 2010
	increased secretion	rotenone and actimycin treatment	Shaham 2009
	increased plasma levels	various MDs	Clarke 2013
	increased plasma levels	various MDs	Alban 2017
	increased plasma levels	MNGIE	Filosto 2018
	increased plasma levels	MILS	Thorburn 2017
	increased plasma levels	COX10 KO mouse	Chen 2018
	decrease	LHON	Morvan 2018
	decrease	LHON	ChaoDeLaBarca 2016
creatine	increase in blood	A354V o C1277STOP en LRPPRC (assembly of CIV) - LSFC	Thompson-Legault 2015
	increase in blood	IOSCA	Buzkova 2018
	increase in blood	various MDs (MELAS, MERRF, mtDNA depletion and deletions)	Shaham 2009
	increased secretion	rotenone treatment	Shaham 2009
	increased unmethylated precursor (GAA+)	PEO	Buzkova 2018
	decrease	LHON	Morvan 2018
	increased creatine/creatinine ratio	IBM	Buzkova 2018
thymidine	increase	MNGIE	Filosto 2018
acylcarnitines	increase	A354V o C1277STOP en LRPPRC (assembly of CIV) - LSFC	Thompson-Legault 2015
	increase	Deletor - FGF21 KO mouse	Forsstrom 2019
	decrease	LHON	ChaoDeLaBarca 2016
	decrease	A354V o C1277STOP en LRPPRC (assembly of CIV) - LSFC	Thompson-Legault 2015

Table 1: Alterations in levels of conventional biomarkers in MDs. The disease/treatment that causes the alteration are indicated.

B. Novel biomarkers

As previously discussed, one of the main problems regarding MDs diagnosis is the lack of specificity and/or sensitivity of the current biomarkers^{2,47}. Discovering new molecules might help to find a better comprehension of the MDs, and for these reasons metabolomics approaches have emerged as a potential tool to precisely diagnose and monitor certain these disorders⁴⁸. To date, a handful of metabolomic studies have been performed in MDs patients and mitochondrial deficiency models, with some metabolites rising as potential biomarkers (see Table 2).

One of the most common metabolic shifts in severe OXPHOS deficiencies is the drop of NAD^+/NADH ratio, which occurs as NAD^+ decreases and NADH accumulates^{40,49,50} (see Table 2). NAD^+ decline is a direct consequence of OXPHOS impairment, as NADH reoxidation mainly depends on the NADH :ubiquinone oxidoreductase (or mitochondrial complex I) (Fig. 1). NAD^+/NADH reductions have been described in NARP/MILS syndrome⁵⁰, IOSCA³⁷, and LS⁴⁰. However, despite being a common feature of MDs, NAD^+/NADH ratio is also present in other metabolic disorders such as type 2 diabetes⁵¹. Therefore, although NAD^+/NADH reduction might be used as an indicator of prevalence of mitochondrial dysfunction, it does not serve as a unique biomarker for diagnosis.

Higher levels of serine have also been reported in multiple MDs, such as IOSCA, PEO, mitochondrial myopathy, encephalomyopathy, MELAS or MIDD³⁷ as well as under mtDNA depletion⁵² (see Table 2). Serine synthesis is derived from glycolysis (specifically from 3-phosphoglycerate)⁵³ (Fig. 5). Serine biosynthesis genes are upregulated under mitochondrial dysfunction⁵², therefore explaining this increase.

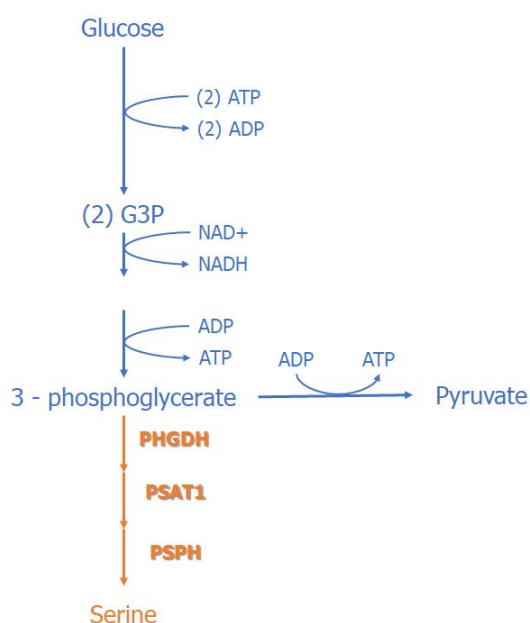


Fig. 5: Scheme of the serine biosynthesis pathway, in orange. Scheme of the glycolysis, in blue. G3P: glyceraldehyde-3-phosphate; PHGDH: D-3-phosphoglycerate dehydrogenase; PSAT1: phosphoserine aminotransferase; PSPH: phosphoserine phosphatase.

Lately, glutamine metabolism has also gained attention as a possible starring biomarker in MDs. Glutamine is converted into glutamate via mitochondrial glutaminase (GLS)⁵⁴.

Glutamate is the most abundant excitatory neurotransmitter, feeds an anaplerotic route into TCA cycle (Fig. 6) and is involved in glutathione (GSH) metabolism. Furthermore, shifting of glutamate transamination reactions is consistent with a drop in the NAD^+/NADH ratio, commonly present in MDs^{35,36}. Moreover, the glutamine-glutamate- α -KG anaplerotic route has been shown to be increased in OXPHOS-defective cell lines⁵⁵ and alterations in glutamine levels have been consistently described in several disorders such as LHON^{42,56}, NARP/MILS⁵⁵ and/or Leigh syndrome⁵⁷ (see Table 2), which strongly supports glutamine-related metabolites as potential biomarkers in MDs.

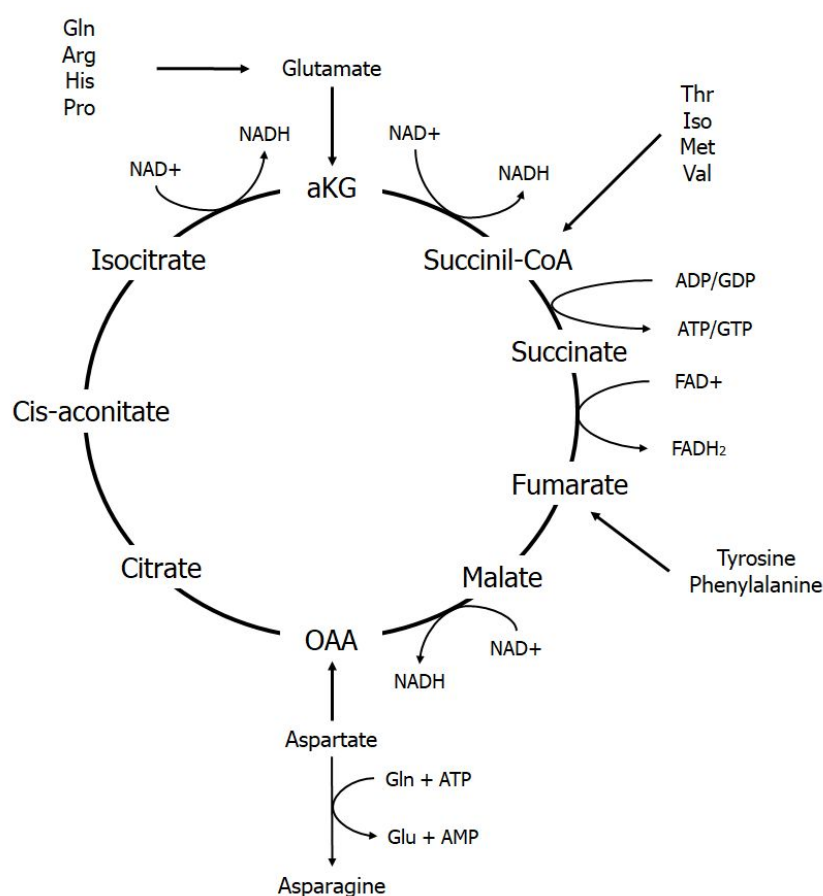


Fig. 6: Scheme of glutamine metabolism. Glutamine is part of an anaplerotic pathway that enters the tricarboxylic acid (TCA) cycle and is metabolized following oxidative (clockwise) or reductive (counterclockwise) carboxylation. OAA: oxaloacetate; aKG: α ketoglutarate; Gln: glutamine; Arg: arginine; His: histidine; Pro: proline; Thr: threonine; Iso: isoleucine; Met: methionine; Val: valine; GTP/ATP: guanosine/adenosine triphosphate; AMP: adenosine monophosphate; NADH: nicotinamide adenine dinucleotide; FADH_2 : flavin adenine dinucleotide.

Another notable change in metabolism in MDs is the reduction observed in aspartate, a central molecule that links several metabolic routes (Fig. 7). On one hand, aspartate depletion promotes rewiring of glutamine metabolism by decreasing feedback inhibition by oxaloacetic acid (OAA) and glutamine-derived aspartate is used as a compensatory force to restore the NAD^+/NADH balance^{50,55}. On the other hand, oxidative carboxylation of glutamine leads to aspartate conversion into alanine and lactate (Fig. 7) thus increasing their levels (see Introduction, Section IV.A)⁵⁵. Altogether, these observations point out to aspartate as a central metabolite in MDs. In keeping with this, aspartate depletion has been shown in LHON^{42,56}, NARP⁵⁰, and LS⁵⁵ as well as in cell models treated with OXPHOS inhibitors, such as rotenone, pierdicin A⁴², phenformin (CI inhibitors)⁵⁸, doxycycline (impairing mitochondrial translation), actinonin (affecting stability of OXPHOS components)⁵⁹ and others (see Table 2).

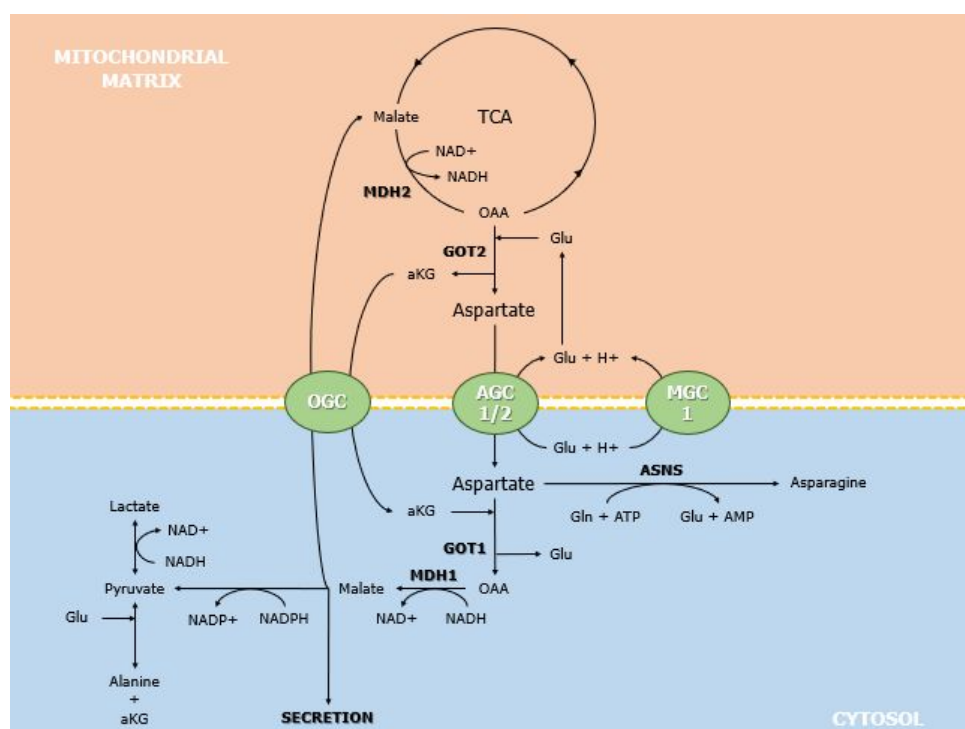


Fig. 7: Scheme of aspartate metabolism. MDH1/2: malate dehydrogenase 1 (cytosolic) and 2 (mitochondrial); GOT1/2: glutamic oxaloacetic transaminase 1 (cytosolic) and 2 (mitochondrial); ASNS: asparagine synthase; AGC1/2: aspartate glutamate carrier 1 (cytosolic) and 2 (mitochondrial); OGC: 2-oxoglutarate carrier; MGC1: mitochondrial glutamate carrier 1; OAA: oxaloacetate; aKG: alpha ketoglutarate; Glu: glutamate; Gln: glutamine; ATP: adenosine triphosphate; AMP: adenosine monophosphate; NADPH: nicotinamide adenine dinucleotide phosphate; NADH: nicotinamide adenine dinucleotide.

Collectively, these findings suggest that alanine, glutamine and aspartate metabolism play a key role in the adaptive changes that happen in cells with OXPHOS impairment and should be strongly considered as a metabolic signature in MDs.

METABOLITE	ALTERATION	ASSOCIATED DISEASE/MUTATION/TREATMENT	PUBLISHED ON
NAD ⁺ /NADH ratio	decrease	various OXPHOS disorders	Lightowers 2015
	decrease	heteroplasmic T8993G mtDNA mutation (mT80) - NARP/MILS syndrome	Gaude 2018
	decrease	A354V o C1277STOP en LRPPRC - LSF	Thompson-Legault 2015
	decrease	rotenone, metformin and antimycin a treatment	Fendt 2013
	decrease	pipecidin+oligomycin treatment	To 2019
	decrease	pipecidin, antimycin and oligomycin treatment	Mootha 2020
	decrease	A3243G mutated cells	Chung 2020
	depletion of NAD ⁺	IOSCA	Buzkova 2018
	increase on NAD ⁺ synthesis	PEO	Buzkova 2018
	increase on NAD ⁺ synthesis	IBM	Buzkova 2018
	decrease	lactate supplementation	Bao 2016
	decrease	rotenone, EtBR	Bao 2016
	increase	AMPK activation with AICAR	Canto 2009
	increase	CCP (despolarización de la membrana)	Bao 2016
serine	increase	mtDNA depletion	Bao 2016
	increase	IOSCA, PEO, MELAS/MIDD	Buzkova 2018
	increase	heteroplasmic T8993G mtDNA mutation (mT80) - NARP/MILS syndrome	Gaude 2018
	increase	Deletor mouse	Nikkanen 2016
	increase	Deletor mouse	Tynismaa 2010
	upregulation of biosynthesis enzymes	actinonin, FCCP, doxycycline and MitoBloCK-6 treatments	Quirós 2017
	downregulation of biosynthesis enzymes	Torin 1 treatment (mTORC1 inhibitor)	Park 2017
	decrease on uptake and cellular consumption	mtDNA depletion	Bao 2016
	decrease	COX10 KO mouse muscle cells	Chen 2018
	decrease	LHON	Morvan 2018
	decrease	LHON	ChaoDeLaBarca 2016
glutamine, aKG	oxidative carboxylation increase	homoplasmic T8993G mtDNA mutation in A6MT - NARP/MILS syndrome	Chen 2018
	oxidative carboxylation predominance	WT and GOT1-KO cells	Birsoy 2015
	reductive carboxylation increase	COX1100 and Cyb100 (parkinsonism/MELAS) cells - lack of OXPHOS function	Chen 2018
	reductive carboxylation increase	heteroplasmic T8993G mtDNA mutation (different heteroplasmy levels)	Gaude 2018
	reductive carboxylation increase	hypoxia and RC inhibitors	Fendt 2013
	reductive carboxylation increase	phenformin treatment (CI inhibitor)	Birsoy 2015
	reductive carboxylation increase	pipecidin and pipecidin+oligomycin treatment	To 2019
	blood glutamine increase	PEO	Buzkova 2018
	increased glutamine	rapamycin	Khan 2017
	decreased glutamine	LHON	ChaoDeLaBarca 2016
	decreased glutamine	LHON	Morvan 2018
aspartate	decreased glutamine	heteroplasmic T8993G mtDNA mutation (mT80) - NARP/MILS syndrome	Gaude 2018
	decreased glutamine and aKG	Ndufs4(KO) mice - Leigh syndrome	Johnson 2020
	decrease	actinonin, FCCP, doxycycline and MitoBloCK-6 treatments	Quirós 2017
	decrease	phenformin treatment (CI inhibitor)	Birsoy 2015
	decrease	heteroplasmic T8993G mtDNA mutation (mT80) - NARP/MILS syndrome	Gaude 2018
	decrease	LHON	ChaoDeLaBarca 2016
	decrease	LHON	Morvan 2018
	decrease	rotenone, pipecidin A treatment	ChaoDeLaBarca 2016
	increase	COX10 KO mouse muscle cells	Chen 2018

Table 2: Alterations on various metabolites in MDs, proposed as potential novel biomarkers. The disease/treatment that causes the alteration is indicated.

V. Mitochondrial dysfunction and stress mechanisms

Each new discovery in the landscape of MDs shows the complexity of its pathophysiology. Several evidences pinpoint that partial or total ATP depletion may not be the sole cause for the wide range of phenotypes observed in MDs¹¹. Therefore, great effort has been made in revealing their underlying mechanisms. Other mechanisms have been proposed, such as overproduction of reactive oxygen species (ROS)^{2,7,11}, metabolic rewiring (see Introduction, Section IV) or mitochondrial biogenesis impairment⁶⁰. Nonetheless, further research has enlightened new key pathways. Here, we have focussed on the latest findings in MDs and cellular stress mechanisms.

A. mTORC1

The role of the mechanistic (mammalian) target of rapamycin complex I (mTORC1) is very interesting in this context. mTORC1 is a nutrient sensor that controls several processes such as protein synthesis, cell growth, *de novo* pyrimidine^{61,62}, purine⁶³ and lipid synthesis, pentose phosphate pathway, and autophagy^{64,65}.

Recent data on a mouse model of mitochondrial depletion⁶⁶, as well as human muscle samples⁶⁷, have shown that mTORC1 is activated in mitochondrial stress. By using the mTORC1 inhibitor rapamycin, Prof. Suomalainen's lab observed that the activation of mTORC1 has a myriad of functions driven by the induction of the activating transcription factor 4 (ATF4)⁶⁶. Hyper-activation of the axis mTORC1-ATF4⁶³ acts as a compensatory mechanism to restore the dNTP pools as well as the metabolic rewiring of pentose phosphate pathways, which are both altered in this model of MDs.

Interestingly, mTORC1 inhibition with rapamycin have also been shown to reduce heteroplasmy by removing defective mitochondria (mitophagy/autophagy) in cell models of MELAS (m.3423G>A/MT-TL1) and LHON (m.11778G>A/p.MT-ND4:R340H)⁶⁸⁻⁷⁰, as well as increase the lifespan and alleviate symptoms in LS (*Ndufs4*^{-/-})^{57,71}, thymidine kinase 2 (TK2) deficiency (Tk2^{KI/KI})⁷² and mitochondrial myopathy (Cox15^{sm/sm})⁷³ mouse models. However, rapamycin has not been effective on other types of MDs⁷⁴, suggesting that mTORC1 might have different roles in the etiology of each disease.

B. Integrated stress response (ISR)

The term ISR was first coined by Ron⁷⁵ & Harding⁷⁶ in order to designate the convergence of different stress responses into the phosphorylation of the alpha subunit of eukaryotic translation initiation factor 2 (eIF2A). Phosphorylation of eIF2A on serine 51 is performed by four eIF2A kinases (Fig. 8), and leads to the blockade of translation initiation of most messenger RNAs (mRNAs) by inhibiting the delivery of the Met-tRNAi to the ternary complex⁷⁷. However, it favours the synthesis of a group of mRNAs that are normally poorly translated because they have two upstream open reading frames (uORFs). A case of these mRNAs with 2 uORFs is the known mitochondrial retrograde signaling agent ATF4⁷⁸ (see Introduction, Section V.C).

Recent research has pinpointed elements of the ISR as having a possible role in MDs. Activation of the PERK/eIF2A axis has been observed in LHON patient fibroblasts⁴² and activation of eIF2A and downstream effectors of the ISR (ATF4, Activating Transcription Factor 5 (ATF5) and C/EBP homologous protein (CHOP)) has been seen in MELAS cell lines⁷⁰. Additionally, activation of the eIF2A downstream target ATF4 occurs in MDs as extensively discussed below (see Introduction, Section V.C). Yet it is still not clear whether ISR activation is beneficial or detrimental to the patients with MDs⁷⁹.

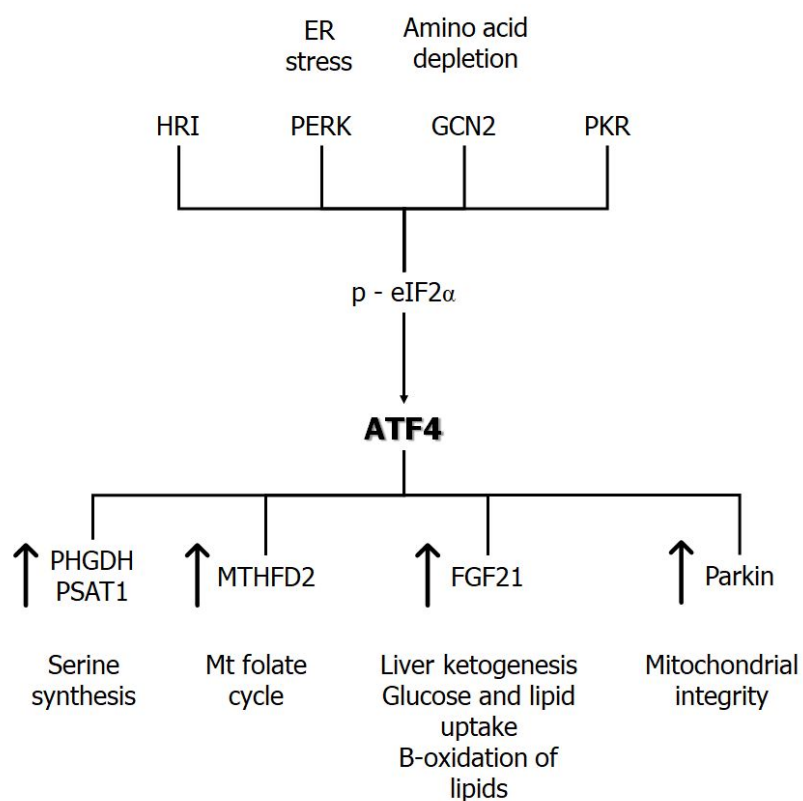


Fig. 8: Scheme of the Integrated Stress Response (ISR). HRI: heme-regulated inhibitor kinase; PERK: protein kinase R-like endoplasmic reticulum kinase; GCN2: general control non-derepressible 2; PKR: protein kinase R; p - eIF2α: phosphorylated eukaryotic translation initiation factor 2 alpha; ATF4: activating transcription factor 4; PHGDH: phosphoglycerate dehydrogenase; PSAT1: phosphoserine aminotransferase 1; MTHFD2: methylenetetrahydrofolate dehydrogenase 2; FGF21: fibroblast growth factor 21.

C. Role ATF4 in MDs

When subjected to stress conditions, mitochondria trigger various signaling pathways within the nucleus activating a transcriptomic response known as retrograde response⁸⁰. Several recent evidence points out to the activation of ATF4 as one of the main regulators in this response⁸¹.

ATF4 belongs to the family of leucine zipper proteins, as it contains a bZIP domain⁸². It can form homodimers or heterodimers with different proteins that modulate its concrete function. It mediates its transcriptional regulator activity through binding to C/EBP-ATF response element (CARE)^{78,83}. ATF4 activation is present in amino acid deprivation⁸⁴, endoplasmic reticulum (ER) stress^{76,78}, cancer⁸⁵ as well as MDs (see below). Furthermore, ATF4 controls the expression of downstream effectors of the ISR and the mitochondrial Unfolded Protein Response (mtUPR)⁸⁶, such as growth arrest and DNA damage-inducible protein (GADD34), CHOP⁷⁸ and ATF5^{66,67}. Additionally, ATF4 controls other genes related to metabolic changes such as asparagine synthase (ASNS)⁸⁷, serine biosynthesis genes, folate cycle genes⁵², fibroblast growth factor 21 (FGF21)^{66,88,89} and Parkin⁹⁰ (Fig. 8) all known to be altered in different forms of MDs. How upregulation of these genes impacts MDs' pathogenesis is unknown and has yet to be investigated.

Several reports have shown ATF4 activation in MDs. It has been reported in cybrids harboring NARP mutations⁸⁷, mouse and human (PEO patients) mitochondrial depletion⁶⁶ and in MELAS cell lines harboring the m.3243G>A mutation.⁷⁰ Furthermore, several groups have observed ATF4 activation under pharmacologically induced mitochondrial dysfunction^{52,59,66,88}. Yet, the upstream regulators of ATF4 are still debatable and might change in different MDs. For instance, mTORC1 is activated in the Deletor mice⁶⁶ and the m.3243G>A cell line⁷⁰. Moreover, mitochondrial stressors induce eIF2A phosphorylation^{59,87}, but no increase is observed in NARP and MELAS cell lines⁸⁷. Further investigation on the molecular mechanisms upstream of ATF4 is needed to unveil the role of these pathways in the pathophysiology of mitochondrial disorders.

Methods

I. Bibliographic research

Literature research was made using the free-access search engine PubMed. At first, key bibliography about mitochondrial disease, metabolomics and mitochondrial stress was provided by Dr. Aurora Gómez-Durán, the leader of the lab. After consulting these references, I was capable of understanding the basics on the field and starting a bibliographic search by myself. Recent publications on the topic and more scientific articles were looked for using keywords and references from other publications. This targeted search provided a more detailed knowledge, along with extensive information. For every publication used, the Impact Factor (IF) of the journal and the number of Citations were consulted. The catalogue was completed with publications provided by Dr. Gómez-Durán.

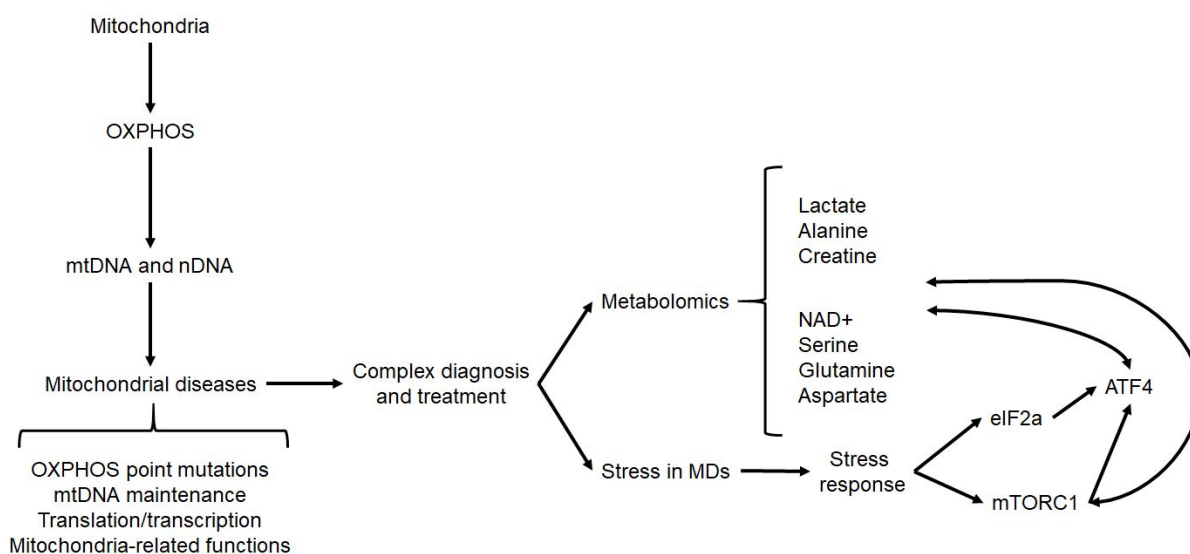


Fig. 9: Scheme of the workflow followed during the bibliographic research.

Keywords for information about mitochondria, OXPHOS and mitochondrial diseases were: 'mitochondria', 'oxidative phosphorylation system', 'OXPHOS', 'electron transport chain', 'mitochondrial DNA', 'mitochondrial genome', 'mitochondrial disease', 'mitochondrial disorder', combining them with the Boolean operator 'AND'.

Keywords for metabolomics in MDs were: 'metabolomics', 'metabolites', 'metabolism', 'amino acid metabolism', 'mitochondria', 'mitochondrial DNA', 'biomarker', combining them with the Boolean operator 'AND'.

Keywords for mitochondrial dysfunction and stress mechanisms were: 'mitochondria', 'mitochondrial disease', 'mitochondrial disorder', 'mitochondrial dysfunction', 'mitochondrial stress', 'integrated stress response', 'activating transcription factor 4', 'ATF4', 'eukaryotic translation initiation factor 2 alpha', 'eIF2a', 'mammalian target of rapamycin complex I', 'mTORC1', combining them with the Boolean operator 'AND'.

II. Cell culturing

Cell lines were a kind gift from the laboratory of Prof. Julio Montoya (University of Zaragoza), full description of the patients and mtDNA sequences of all the cell lines is described elsewhere⁹¹. Cell lines were grown in supplemented medium (SM) containing Dulbecco's modified eagle medium (DMEM) containing glucose (4.5 g/l), pyruvate (0.11 g/l) (Gibco, ref.: 41966_029), uridine (100ug/ml) and fetal bovine serum (FBS) (5 %) (Gibco, ref.: 10270_106) without antibiotics at 37°C and 5% CO₂ conditions. All the experiments were performed in at least 2 technical repeats.

Defrosting cells. Cells were transferred from cryovials into Falcon tubes containing 4-5 mL of SM. Cells were centrifuged at 1200g for 5 min and supernatant was discarded. The pellet was then resuspended in SM and cells were seeded in 100mm plates containing 8-10 mL of SM, then incubated at 37°C and 5% CO₂ until confluence was reached.

Passing cells. When cells reached ~90% confluence the medium was discarded and the plate was washed with PBS. PBS was discarded and 1 mL of trypsin-EDTA (0.05%) (Gibco, 2300_054) was added to detach the cells from the plate. Cells were put back in the incubator at 37°C and 5% CO₂ for 3-5 min. Cells were observed at the microscope to check for dettaching. To stop trypsinization, cells were resuspended in SM by pipetting up and down, and after that were transferred to a new plate with a fresh SM. Cells were then incubated at 37°C and 5% CO₂ until the desired confluence level was reached.

Freezing cells. Cells were trypsinized as described previously. After detaching, cells were centrifuged at 1200g for 5 min and supernatant was discarded. After centrifugation, pellets

were resuspended with freezing media (FM) composed of FBS and dimethylsulfoxide (DMSO) (10%) at $1.5\text{--}3 \times 10^6$ cells/ml. DMSO is a cryoprotectant that must be added in order to prevent cells from death due to formation of water crystals. Approximately, 1 mL of the mixture of resuspended cells in FM was transferred to each cryovial. Quickly after that the cryovials were stored at -80°C in expanded polystyrene boxes to allow a progressive decrease in temperature by $1^{\circ}\text{C}/\text{hour}$ and thus cryopreservation of the cells. The day after the frozen cryovials and then transferred to the liquid nitrogen ($\text{N}_{2(l)}$) for long term storage.

III. Denaturing electrophoresis and Western blot analysis.

Protein extraction and quantification. Total protein extracts were prepared according to each protein's solubilities. Protein extracted for kinase phosphorylation analysis was extracted using PathScan® Sandwich ELISA Lysis Buffer from Cell signaling. Protein concentrations were measured using Bradford reagent and following manufacturer's conditions.

Electrophoresis. In any case protein extracts (30ug) were loaded on NuPAGE® Bis-Tris Precast Midi Protein Gels with MES (Invitrogen®) with 26 wells. Electrophoresis was carried out following the manufacturer's conditions. SeeBlue® Plus2 Pre-stained Protein Standard from Invitrogen® was used in each electrophoresis as protein size markers.

Transfer. The separated proteins were transferred to polyvinylidene fluoride membranes using the iBLOT system (Invitrogen®) or Mini Trans-Blot® transfer system from Biorad®.

Immunoblotting and detection. The resulting blots were blocked for 1 h with 5% nonfat dry milk in Tris-Buffered Saline, 0.1% TWEEN® 20 (TBST) and probed overnight at 4°C with primary antibodies in TBST with 5% Bovine serum albumin (BSA) or nonfat dry milk using the appropriate concentration as per the manufacturer's conditions with small adaptations (Table 3). After the primary antibody, blots were incubated for 1 h with secondary antibodies in TBST with 5% BSA (Bovine serum albumin or nonfat dry milk) conjugated with horseradish peroxidase (HRP) and immuno-detected using an Amersham Imager 600.

Immunoblotting imaging and quantification. The bands for each antibody were quantified, aligned and cropped using the Fiji program and the OD was used as a value for statistical

purposes. In order to avoid inter-blot variation one cell line was used as an internal control and the values of the OD corrected by β -Actin were relative to it in each case.

Antibody	Code	Commercial	Concentration
4EBP1	ab32130	Abcam	1 in 1000
Phospho-4EBP1 ^{Ser65}	9451	Cell signalling	1 in 500
EIF2A	9722	Cell signalling	1 in 500
Phospho-EIF2A ^{Ser51} (D9G8)	3398	Cell signalling	1 in 500
IRE1a	3294T	Cell signalling	1 in 500
PERK	5683T	Cell signalling	1 in 500
BIP	3177T	Cell signalling	1 in 500
ATF5	ab184923	Abcam	1 in 1000
ATF4	sc-390063	Santa Cruz Biotechnology	1 in 500
HSP10	sc-376313	Santa Cruz Biotechnology	1 in 500
B-Actin	a1978	Sigma	1 in 2000
Vinculin	V4505	Sigma	1 in 1000

Table 3: Antibodies used for immunodetection of proteins. The commercial, its code and concentration are indicated.

IV. Real-time PCR quantification of transcripts.

Total RNA was isolated from cells exponentially growing using an RNA isolation kit from Qiagen® according to the manufacturer's protocol. Quantification of mRNA by real-time PCR (RT-PCR) was carried out using the High capacity cDNA reverse transcription kit (Applied Biosystems) following the manufacturer's conditions. The mRNA levels were determined using probes from Applied Biosystems and following MQIE guidelines⁹². The expression levels were normalized with glyceraldehyde-3-phosphate dehydrogenase (GADPH) and B-ACTIN as housekeeping genes. The codes of each of the probes are included in Table 4. The comparative C_q method was used for relative quantification of gene expression.

Differences in the Cq values (dCq) of the transcript of interest and the reference gene were used to determine the relative expression of the gene in each sample. The ddCq method was used to calculate the fold change (FC) of expression compared to the controls.

Name	Description	Product Number
ACTB	actin beta	Hs01060665_g1
ATF4	activating transcription factor 4	Hs00909569_g1
ATF5	activating transcription factor 5	Hs01119208_m1
ATF6	activating transcription factor 6	Hs00232586_m1
GAPDH	glyceraldehyde-3-phosphate dehydrogenase	Hs02786624_g1

Table 4: Probes used for RT-qPCR amplification. Product number of each probe is indicated.

V. Statistical analysis and graphics

Graphics were created with Excel. In the Western blot quantification, relative protein levels corrected by loading control are shown. Graphics show mean values \pm standard deviation (SD) of the technical replicates.

Statistical analysis and graphic design was performed using Excel. Mean values of each technical replicate were compared using 1 factor ANOVA with a level of significance of $p < 0.05$. Then, unpaired t-student tests of each variant vs. control were performed with a level of significance of $p < 0.05$.

Results

Case-study: Unmasking the mechanisms of stress in cell lines with mutations causing LHON.

Leber's Hereditary Optic Neuropathy (LHON) is a mitochondrial disorder (MD) caused by mutations in the mitochondrial genome (mtDNA). Usually these mutations sit on genes encoding subunits of the complex I of the oxidative phosphorylation system (OXPHOS) - the system responsible for the synthesis of energy of the cell. The three commonest mutations causing LHON are non-synonym changes (see Section III.A)¹².

LHON is characterized by a central vision loss due to degeneration of retinal ganglion cells (RGCs). Being caused by mutations in the mtDNA, LHON is maternally inherited, but it's penetrance is incomplete as not all the carriers of the mutation develop the disease, which affects mostly young males. Moreover, environmental and mtDNA genetic factors also contribute to this variability but are not enough to explain it. The exact pathophysiological mechanism of the disease is yet unknown. Thus, other compensatory mechanisms might act as potential candidates to answer this question.

Recent observations in models of MDs such as the mutated Twinkle helicase (model of mtDNA deletions)⁶⁶, Ndufs4 KO mouse (model of complex I dysfunction)⁵⁷ have shown different responses of cellular stress which might be related with the metabolic rewiring observed in these disorders. Most of the observations have proposed a link between the mitochondrial dysfunction and the activation of the integrated stress response (ISR) as well as mitochondrial unfolded protein response (mtUPR)⁶⁶. Discovering how these processes are involved in the pathogenesis of LHON and other MDs would enlighten the way to understanding its complexity and finding new therapeutic options.

A. eIF2A is activated in m.3460G>A

The activation of the eukaryotic translation initiation factor 2 alpha (eIF2A) is the common point in which the different activators (HRI, PKR, PERK and GCN2) of the ISR converge⁷⁸. As

eIF2A is activated in mitochondrial stress^{42,59}, we decided to check its phosphorylation state in LHON cell lines.

We observed that eIF2A activation is increased in cell lines carrying the m.3460G>A/ p.MT-ND1:A52T mutation but not in cells carrying m.11778G>A/ p. MT-ND4:R340H. Given that the observed p-value is almost 0.05 ($p=0.0675$), but we consider that further experiments are needed to refuse the hypothesis in this case.

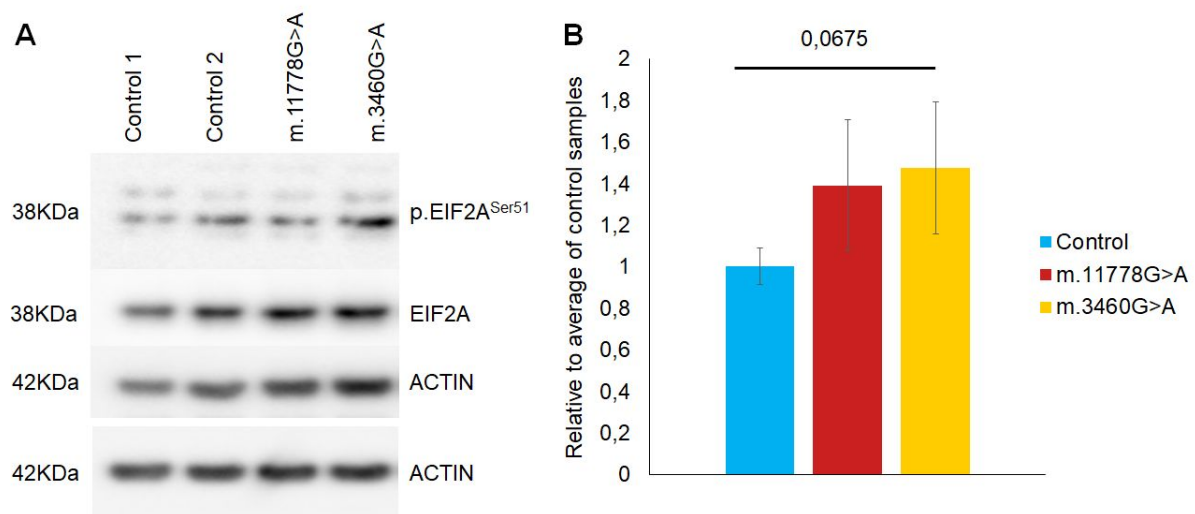


Fig. 10: Quantification of p.eIF2A^{Ser51} in LHON cell lines compared to control.

A) Immunodetection of eIF2A: eukaryotic initiation factor 2 alpha subunit and its phosphorylated form p.eIF2A. Gels were run, transferred and immunoblotted simultaneously using B-Actin as loading control. Size and name of each protein are indicated.

B) Relative quantification (to average of controls) of the levels of p.eIF2A^{Ser51} protein corrected by loading are shown. Levels correspond to phosphorylated/non-phosphorylated ratio. Two control cell lines and one cell line per LHON variant were analysed. The data represents 3 independent technical experiments for each cell line \pm standard deviation (SD) of the mean. Statistical testing was performed by using a 1-way-ANOVA test followed by unpaired t-test to compare each mutant to the controls. Exact p-values corrected for t-student are indicated.

B. mTORC1 is activated in m.11778G>A

mTORC1 is a nutrient sensor that controls cell growth and protein synthesis, and other cellular processes such as autophagy, the pentose phosphate pathway and *de novo* nucleotide and lipid synthesis^{64,65}. Studies on MDs models have shown activation of mTORC1 is activated in LHON⁷¹, Leigh syndrome⁹³, mitochondrial myopathy^{66,73} and thymidine kinase 2 deficiency⁷². Moreover, it's been shown that mTORC1 controls ATF4 expression and translation through 4EBP1⁹⁴. 4EBP1 is a downstream target of mTORC1. Thus, we measured the levels of activation as a surrogate of mTORC1 activation in LHON cell lines.

We saw a significant activation of 4EBP1 in cells carrying the m.11778G>A/ p.MT-ND4:R340H mutation, but not in those carrying m.3460G>A/ p.MT-ND1:A52T. 4EBP1 is activated by mTORC1, so 4EBP1 activation reflects an increase in mTORC1 activity.

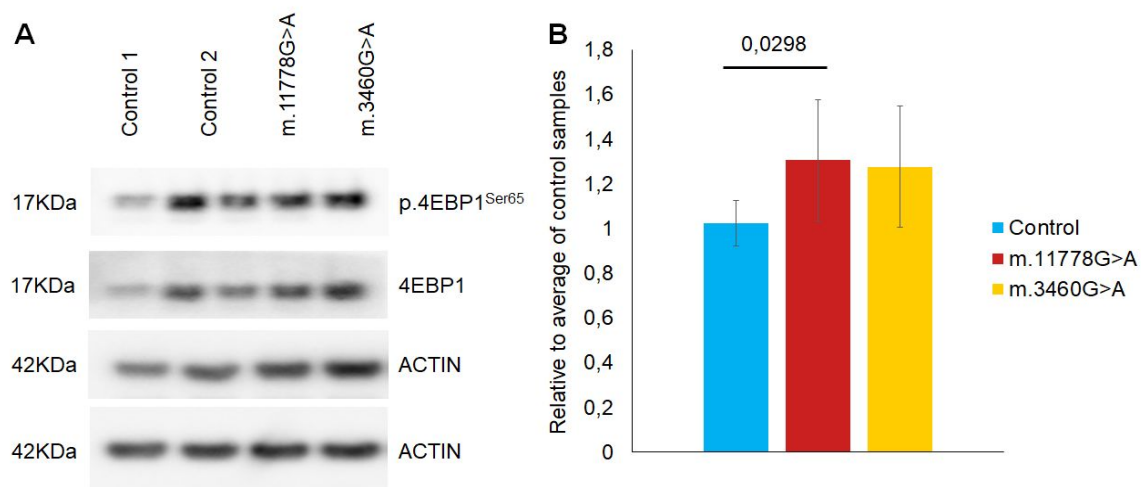


Fig. 11: Quantification of p.4EBP1^{Ser65} in LHON cell lines compared to control.

A) Immunodetection of 4EBP1: EIF4E binding protein 1 and its phosphorylated form p.4EBP1^{Ser65}. Gels were run, transferred and immunoblotted simultaneously using B-Actin as loading control. Size and name of each protein are indicated.

B) Relative quantification (to average of controls) of the levels of p.4EBP1^{Ser65} protein corrected by loading are shown. Levels correspond to phosphorylated/non-phosphorylated ratio. Two control cell lines and one cell line per LHON variant were analysed. The data represents 3 independent technical experiments for each cell line \pm standard deviation (SD) of the mean. Statistical testing was performed by using a 1-way-ANOVA test followed by unpaired t-test to compare each mutant to the controls. Exact p-values corrected for unpaired t-student are indicated.

C. No differences are observed in PERK levels

PERK is one of the four eIF2A kinases and mainly responds to ER stress⁷⁸. As eIF2A is activated in cell lines carrying the m.3460G>A/ p.MT-ND1:A52T mutation, we asked if this activation derives from ER stress or other stimuli.

Furthermore, PERK activation has been previously observed in LHON⁴². In contrast with this, we have found no changes in PERK levels in LHON cell lines (Fig. 12).

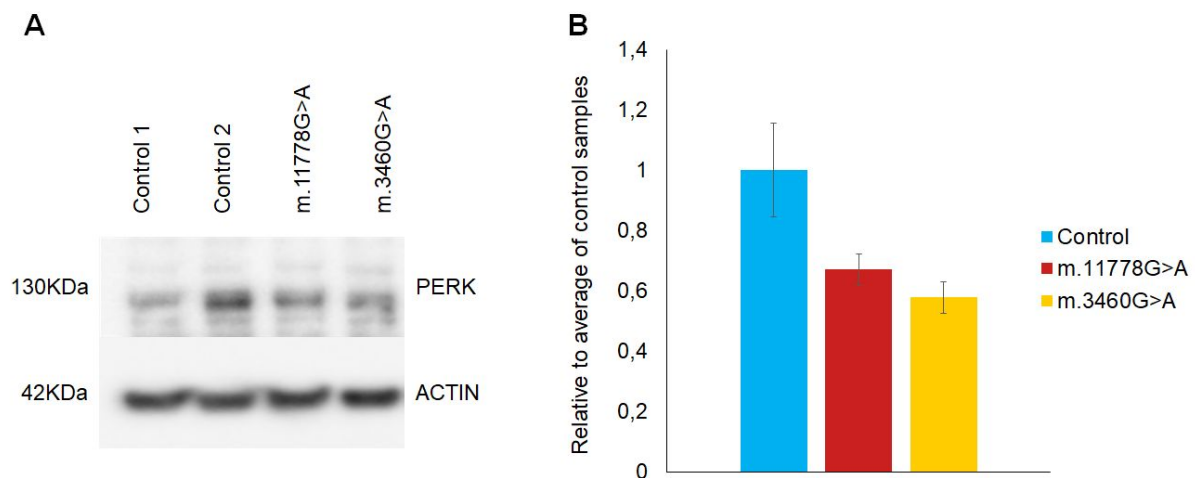


Fig. 12: Quantification of PERK in LHON cell lines compared to control.

A) Immunodetection of PERK: protein kinase R-like ER kinase. Gels were run, transferred and immunoblotted simultaneously using B-Actin as loading control. Size and name of each protein are indicated.

B) Relative quantification (to average of controls) of the levels of PERK protein corrected by loading are shown. Two control cell lines and one cell line per LHON variant were analysed. The data represents 2 independent technical experiments for each cell line \pm standard deviation (SD) of the mean. Statistical testing was performed by using a 1-way-ANOVA test followed by unpaired t-test to compare each mutant to the controls. Exact p-values corrected for unpaired t-student are indicated.

D. mtUPR is not activated in LHON cell lines

Under stressful conditions such as ER stress⁹⁵ or amino acid deprivation⁸⁴, ATF4 translation is activated by p.eIF2A. ATF4 is the best characterized effector of the ISR and regulates genes such as CHOP, ATF3, ASNS or GADD34⁷⁸. Furthermore, ATF4 has a suspected role in MDs as mitochondrial dysfunction leads to ATF4 activation^{52,59,87}. This involvement could be key in the metabolic rewiring that cells undergo in MDs, as it induces changes in amino acid uptake and biosynthesis, the folate cycle, FGF21 and autophagy (see Introduction, Section V.C). One of the effects of ATF4 activation is the triggering of the mtUPR. HSP10 and ATF5 are effectors of the mtUPR⁸⁶. As eIF2A is activated, we checked for ATF4 and mtUPR protein levels in LHON cell lines.

We did not observe changes on protein levels of ATF4 or its downstream targets ATF5 and HSP10 (Fig. 13).

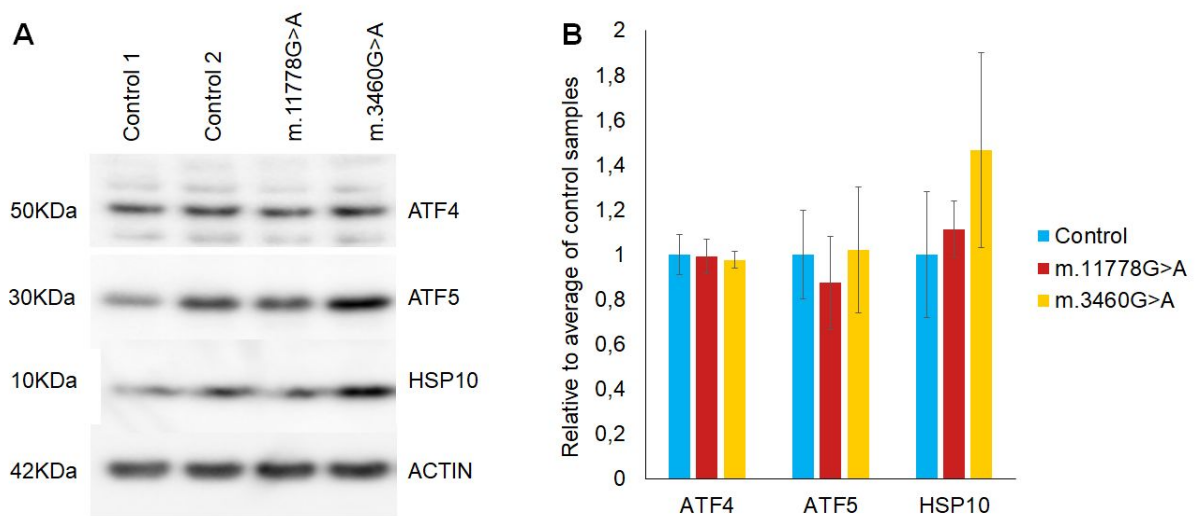


Fig. 13: Quantification of mtUPR proteins in LHON cell lines compared to control.

A) Immunodetection of ATF4: activating transcription factor 4; ATF5: activating transcription factor 5; HSP10: heat-shock 10 kDa protein. Gels were run, transferred and immunoblotted simultaneously using B-Actin as loading control. Size and name of each protein are indicated.

B) Relative quantification (to average of controls) of the levels of protein corrected by loading are shown. Two control cell lines and one cell line per LHON variant were analysed. The data represents 2 independent technical experiments for each cell line \pm standard deviation (SD) of the mean. Statistical testing was performed by using a 1-way-ANOVA test followed by unpaired t-test to compare each mutant to the controls. Exact p-values corrected for unpaired t-student are indicated.

E. ATF4 is transcriptionally downregulated in m.3460G>A cell line

Apart from being translationally regulated by eIF2A and in an mTORC1-dependent manner, ATF4 is also transcriptionally upregulated by mTORC1⁹⁴. We showed no changes on ATF4 protein levels (see Results, Section D) in any of the LHON cell lines compared to the controls and so studied the mRNA levels in order to know if they might follow a different trend. We also measured the levels of transcripts ATF3, a known downstream target of ATF4 involved in MDs⁶⁷.

We observed a significant downregulation of the levels of mRNA of ATF4 in cell lines carrying the m.3460G>A/ p.MT-ND1:A52T mutation, but not on those carrying m.11778G>A/ p. MT-ND4:R340H. Yet, no differences in ATF3 mRNA levels were observed in any of the LHON cell lines (Fig. 14).

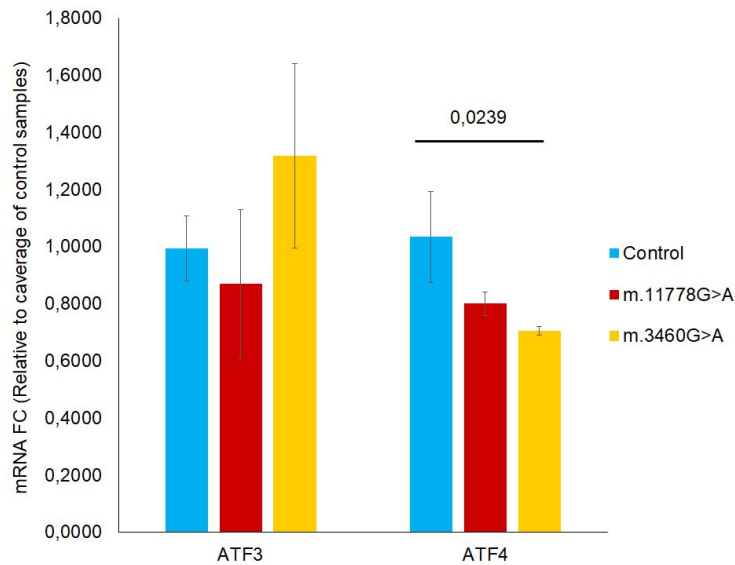


Fig. 14: mRNA fold change of ATF3 and 4 in LHON cell lines compared to control. Three control cell lines and one cell line per LHON mutation were analyzed. Data represents 3 independent technical replicates for each cell line \pm standard deviation (SD) of the mean. Statistical testing was performed by using a 1-way-ANOVA test followed by unpaired t-test to compare each mutant to the controls. Exact p-values corrected for unpaired t-student are indicated.

F. ER stress is not activated in cell lines carrying LHON mutations

ER stress is not only sensed by PERK, but also by IRE1a and ATF6⁹⁶. As PERK signalling is not activated in LHON, we asked whether other PERK-independent ER stress upstream regulators were responsible for the eIF2A activation.

In keeping with the previous findings in PERK (see Results, Section C) we did not see any changes in the labels of proteins of protein IRE1a and ER stress effector BiP in LHON cell lines compared to the controls (Fig. 15) or the levels of expression of ATF6 (Fig.16).

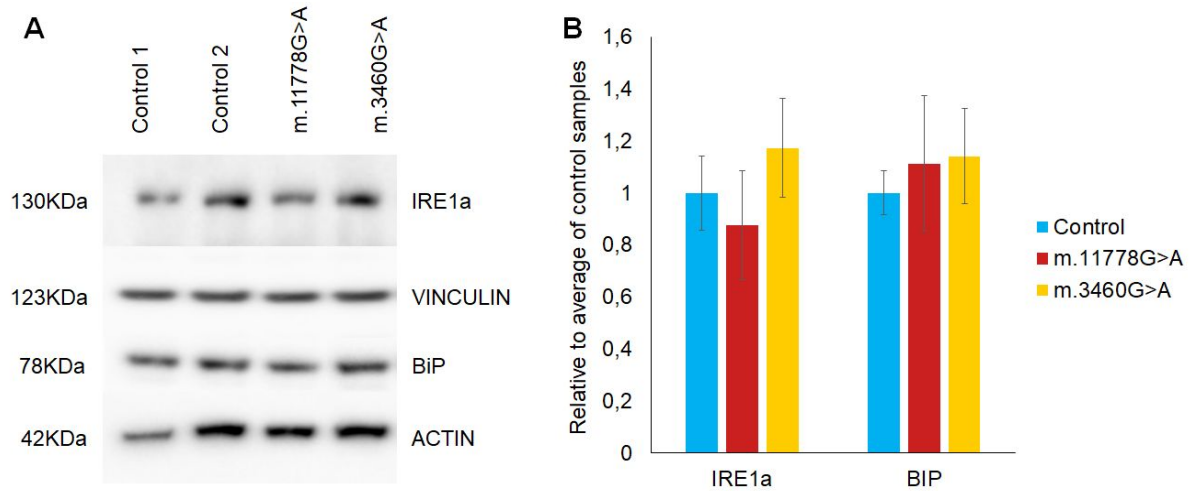


Fig. 15: Quantification of ER stress proteins in LHON cell lines compared to control.

A) Immunodetection of IRE1a: serine/threonine-protein kinase/endoribonuclease IRE1a; BiP: binding immunoglobulin protein. Gels were run, transferred and immunoblotted simultaneously using B-Actin and Vinculin as loading controls. Size and name of each protein are indicated.

B) Relative quantification (to average of controls) of the levels of protein corrected by loading are shown. Two control cell lines and one cell line per LHON variant were analysed. The data represents 2 independent technical experiments for each cell line \pm standard deviation (SD) of the mean. Statistical testing was performed by using a 1-way-ANOVA test followed by unpaired t-test to compare each mutant to the controls. Exact p-values corrected for unpaired t-student are indicated.

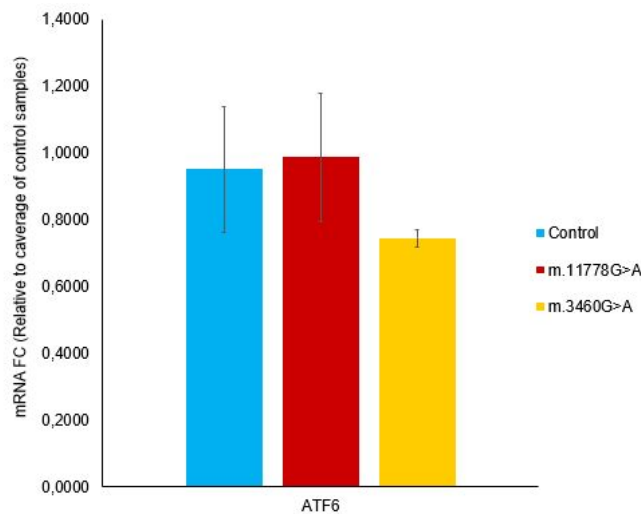


Fig. 16: mRNA fold change of ATF6 in LHON cell lines compared to control. Three control cell lines and one cell line per LHON mutation were analyzed. Data represents 3 independent technical replicates for each cell line \pm standard deviation (SD) of the mean. Statistical testing was performed by using a 1-way-ANOVA test followed by unpaired t-test to compare each mutant to the controls. Exact p-values corrected for unpaired t-student are indicated.

Discussion and conclusions

Here, we studied the mRNA and protein levels of some stress-related proteins in two different mutations causing the disease of LHON. We aimed to understand whether a deregulation of these pathways is involved in the pathogenesis of the disease. We focused on pathways related with MDs such as mTORC1 and the axis PERK/eIF2a/ATF4 axis, both being found to be altered under MDs.

First, we checked the levels of 4EBP1, a downstream target of mTORC1, whose phosphorylation state reflects mTORC1 activation and controls transcriptionally^{66,94} and translationally the levels of the mito-stress sensor ATF4⁹⁴. Similar to previous observations in the mutated Twinkle helicase⁶⁶ and *Ndufs4*-KO⁵⁷ mouse model, we found that mTORC1 is activated in the cell lines carrying the mutation m.11778G>A/ p. MT-ND4:R340H, but not on those carrying the m.3460G>A/ p.MT-ND1:A52T, suggesting a mutation-specific phenotype. Indeed, while the m.3460G>A/ p.MT-ND1:A52T variant produces a 70% decrease in complex I activity, the m.11778G>A/ p. MT-ND4:R340H does not affect it⁹⁷, implying a possible correlation between the complex deficiency and the activation of mTORC1 that needs to be further studied.

eIF2A activation is a common hallmark in mitochondrial stress^{42,59}. In keeping with previous findings, we observed an increased activation of eIF2A (see Results, Section A) in the cell lines carrying the m.3460G>A/ p.MT-ND1:A52T variant, supporting the mutation-specific stress response hypothesis. This phosphorylation state of eIF2A might be induced by several upstream signals such as heme-regulated eIF2a kinase 1 (HRI), protein kinase R (PKR) or general control non-derepressible 2 (GCN2) and PERK. We did not find differences in PERK levels (see Results, Section C) in any of the LHON mutations, contrary to previous findings in LHON fibroblasts⁴², pointing towards another mechanism that will be evaluated further on.

Next, we studied whether the downstream effectors of eIF2A and mTORC1 were also differentially regulated. We focussed on ATF4 and its downstream targets such as ATF3⁶⁷, ATF5^{66,67} and HSP10 as they are widely associated with MDs and the mtUPR^{59,66,67}. Surprisingly, we did not see any changes in the levels of proteins and mRNA of all the

downstream targets of ATF4 suggesting that mtUPR is not activated in LHON cell lines. We did, however, observe a striking decrease in the ATF4 mRNA levels in the cell lines carrying the m.3460G>A/ p.MT-ND1:A52T that needs to be further studied.

Lastly, we investigated if other targets of the endoplasmic reticulum (ER) stress independent of PERK, such as IRE1a and ATF6 and its downstream target BIP, were activated by the LHON mutations. In agreement with PERK levels, there were no changes in the ATF6 mRNA levels and the protein levels of IRE1a and BiP (see Results, Section F). These findings confirm the absence of ER stress driven by LHON mutations.

All together, our observations indicate a mutation specific stress response in each of the LHON mutations that needs to be further studied. Identifying all the involved elements and their impact in LHON pathogenesis is a key step to propose new drugs for treating the disease. In the future, more differences between mutations affecting other OXPHOS complexes or other aspects of mitochondrial functioning such as mtDNA maintenance and protein synthesis might be discovered.

Bibliography

1. Tilokani, L., Nagashima, S., Paupe, V. & Prudent, J. Mitochondrial dynamics: overview of molecular mechanisms. *Essays Biochem.* **62**, 341–360 (2018).
2. Gorman, G. S. *et al.* Mitochondrial diseases. *Nat. Rev. Dis. Primer* **2**, 16080 (2016).
3. Mathews, C. K., Holde, K. E. V. & Appling, D. R. *Bioquímica (4a. ed.)*. (Pearson Educación, 2013).
4. Hagstrom, E., Freyer, C., Battersby, B. J., Stewart, J. B. & Larsson, N.-G. No recombination of mtDNA after heteroplasmy for 50 generations in the mouse maternal germline. *Nucleic Acids Res.* **42**, 1111–1116 (2014).
5. Genomics England Research Consortium *et al.* Nuclear-mitochondrial DNA segments resemble paternally inherited mitochondrial DNA in humans. *Nat. Commun.* **11**, 1740 (2020).
6. Timmis, J. N., Ayliffe, M. A., Huang, C. Y. & Martin, W. Endosymbiotic gene transfer: organelle genomes forge eukaryotic chromosomes. *Nat. Rev. Genet.* **5**, 123–135 (2004).
7. Hahn, A. & Zuryn, S. The Cellular Mitochondrial Genome Landscape in Disease. *Trends Cell Biol.* **29**, 227–240 (2019).
8. Calvo, S. E., Clauser, K. R. & Mootha, V. K. MitoCarta2.0: an updated inventory of mammalian mitochondrial proteins. *Nucleic Acids Res.* **44**, D1251–D1257 (2016).
9. Lightowlers, R. N., Taylor, R. W. & Turnbull, D. M. Mutations causing mitochondrial disease: What is new and what challenges remain? *Science* **349**, 1494–1499 (2015).
10. Chinnery, P. F. Mitochondrial disease in adults: what's old and what's new? *EMBO Mol. Med.* **7**, 1503–1512 (2015).
11. Suomalainen, A. & Battersby, B. J. Mitochondrial diseases: the contribution of organelle stress responses to pathology. *Nat. Rev. Mol. Cell Biol.* **19**, 77–92 (2018).

12. Online Mendelian Inheritance in Man, OMIM®. Johns Hopkins University, Baltimore, MD.
MIM Number: 535000. 7 September 2020. World Wide Web URL: <https://omim.org/>.
13. Leber, Th. Ueber hereditäre und congenital-angelegte Sehnervenleiden. *Albrecht Von Graefes Arch. Für Ophthalmol.* **17**, 249–291 (1871).
14. Yu-Wai-Man, P., Griffiths, P. G. & Chinnery, P. F. Mitochondrial optic neuropathies – Disease mechanisms and therapeutic strategies. *Prog. Retin. Eye Res.* **30**, 81–114 (2011).
15. Online Mendelian Inheritance in Man, OMIM®. Johns Hopkins University, Baltimore, MD.
MIM Number: 256000: 7 September 2020. World Wide Web URL: <https://omim.org/>.
16. Lake, N. J., Compton, A. G., Rahman, S. & Thorburn, D. R. Leigh syndrome: One disorder, more than 75 monogenic causes: Leigh Syndrome. *Ann. Neurol.* **79**, 190–203 (2016).
17. Nesbitt, V. *et al.* The UK MRC Mitochondrial Disease Patient Cohort Study: clinical phenotypes associated with the m.3243A>G mutation--implications for diagnosis and management. *J. Neurol. Neurosurg. Psychiatry* **84**, 936–938 (2013).
18. Thorburn, D. R., Rahman, J. & Rahman, S. Mitochondrial DNA-Associated Leigh Syndrome and NARP. in *GeneReviews*® (eds. Adam, M. P. *et al.*) (University of Washington, Seattle, 1993).
19. D'Aurelio, M., Vives-Bauza, C., Davidson, M. M. & Manfredi, G. Mitochondrial DNA background modifies the bioenergetics of NARP/MILS ATP6 mutant cells. *Hum. Mol. Genet.* **19**, 374–386 (2010).
20. Online Mendelian Inheritance in Man, OMIM®. Johns Hopkins University, Baltimore, MD.
MIM Number: 540000: 7 September 2020. World Wide Web URL: <https://omim.org/>.
21. El-Hattab, A. W., Adesina, A. M., Jones, J. & Scaglia, F. MELAS syndrome: Clinical manifestations, pathogenesis, and treatment options. *Mol. Genet. Metab.* **116**, 4–12

- (2015).
22. Klein Gunnewiek, T. M. *et al.* m.3243A > G-Induced Mitochondrial Dysfunction Impairs Human Neuronal Development and Reduces Neuronal Network Activity and Synchronicity. *Cell Rep.* **31**, 107538 (2020).
 23. Online Mendelian Inheritance in Man, OMIM®. Johns Hopkins University, Baltimore, MD. MIM Number: 520000: 7 September 2020. World Wide Web URL: <https://omim.org/>.
 24. Murphy, R., Turnbull, D. M., Walker, M. & Hattersley, A. T. Clinical features, diagnosis and management of maternally inherited diabetes and deafness (MIDD) associated with the 3243A>G mitochondrial point mutation. *Diabet. Med.* **25**, 383–399 (2008).
 25. Grady, J. P. *et al.* mt DNA heteroplasmy level and copy number indicate disease burden in m.3243A>G mitochondrial disease. *EMBO Mol. Med.* **10**, (2018).
 26. Picard, M. & Hirano, M. Disentangling (Epi)Genetic and Environmental Contributions to the Mitochondrial 3243A>G Mutation Phenotype: Phenotypic Destiny in Mitochondrial Disease? *JAMA Neurol.* **73**, 923 (2016).
 27. Pickett, S. J. *et al.* Phenotypic heterogeneity in m.3243A>G mitochondrial disease: The role of nuclear factors. *Ann. Clin. Transl. Neurol.* **5**, 333–345 (2018).
 28. Nikali, K. *et al.* Infantile onset spinocerebellar ataxia is caused by recessive mutations in mitochondrial proteins Twinkle and Twinky. *Hum. Mol. Genet.* **14**, 2981–2990 (2005).
 29. Pirinen, E. *et al.* Niacin Cures Systemic NAD⁺ Deficiency and Improves Muscle Performance in Adult-Onset Mitochondrial Myopathy. *Cell Metab.* **31**, 1078-1090.e5 (2020).
 30. Spinelli, J. B. & Haigis, M. C. The multifaceted contributions of mitochondria to cellular metabolism. *Nat. Cell Biol.* **20**, 745–754 (2018).
 31. Haas, R. H. *et al.* Mitochondrial Disease: A Practical Approach for Primary Care Physicians. *PEDIATRICS* **120**, 1326–1333 (2007).

32. Debray, F.-G. *et al.* Diagnostic Accuracy of Blood Lactate-to-Pyruvate Molar Ratio in the Differential Diagnosis of Congenital Lactic Acidosis. *Clin. Chem.* **53**, 916–921 (2007).
33. Haas, R. H. *et al.* The in-depth evaluation of suspected mitochondrial disease. *Mol. Genet. Metab.* **94**, 16–37 (2008).
34. Parikh, S. *et al.* Diagnosis and management of mitochondrial disease: a consensus statement from the Mitochondrial Medicine Society. *Genet. Med.* **17**, 689–701 (2015).
35. Uittenbogaard, M. & Chiaramello, A. Mitochondrial Respiratory Disorders: A Perspective on their Metabolite Biomarkers and Implications for Clinical Diagnosis and Therapeutic Intervention. *Biomark. J.* **1**, (2015).
36. Clarke, C. *et al.* Mitochondrial respiratory chain disease discrimination by retrospective cohort analysis of blood metabolites. *Mol. Genet. Metab.* **110**, 145–152 (2013).
37. Buzkova, J. *et al.* Metabolomes of mitochondrial diseases and inclusion body myositis patients: treatment targets and biomarkers. *EMBO Mol. Med.* **10**, (2018).
38. Haas, R. H. Thiamin and the Brain. *Annu. Rev. Nutr.* **8**, 483–515 (1988).
39. Wyss, M. & Kaddurah-Daouk, R. Creatine and Creatinine Metabolism. *Physiol. Rev.* **80**, 1107–1213 (2000).
40. Thompson Legault, J. *et al.* A Metabolic Signature of Mitochondrial Dysfunction Revealed through a Monogenic Form of Leigh Syndrome. *Cell Rep.* **13**, 981–989 (2015).
41. Shaham, O. *et al.* A plasma signature of human mitochondrial disease revealed through metabolic profiling of spent media from cultured muscle cells. *Proc. Natl. Acad. Sci.* **107**, 1571–1575 (2010).
42. Chao de la Barca, J. M. *et al.* The metabolomic signature of Leber’s hereditary optic neuropathy reveals endoplasmic reticulum stress. *Brain* **139**, 2864–2876 (2016).
43. Smeitink, J. A., Zeviani, M., Turnbull, D. M. & Jacobs, H. T. Mitochondrial medicine: A metabolic perspective on the pathology of oxidative phosphorylation disorders. *Cell*

- Metab.* **3**, 9–13 (2006).
44. Alban, C., Fatale, E., Joulani, A., Ilin, P. & Saada, A. The Relationship between Mitochondrial Respiratory Chain Activities in Muscle and Metabolites in Plasma and Urine: A Retrospective Study. *J. Clin. Med.* **6**, 31 (2017).
 45. Koga, Y. *et al.* Molecular pathology of MELAS and l-arginine effects. *Biochim. Biophys. Acta BBA - Gen. Subj.* **1820**, 608–614 (2012).
 46. Filosto, M. *et al.* Mitochondrial Neurogastrointestinal Encephalomyopathy (MNGIE-MTDPS1). *J. Clin. Med.* **7**, 389 (2018).
 47. Rahman, J. & Rahman, S. Mitochondrial medicine in the omics era. *The Lancet* **391**, 2560–2574 (2018).
 48. Steele, H. E., Horvath, R., Lyon, J. J. & Chinnery, P. F. Monitoring clinical progression with mitochondrial disease biomarkers. *Brain* **140**, 2530–2540 (2017).
 49. Fendt, S.-M. *et al.* Reductive glutamine metabolism is a function of the α -ketoglutarate to citrate ratio in cells. *Nat. Commun.* **4**, 2236 (2013).
 50. Gaude, E. *et al.* NADH Shuttling Couples Cytosolic Reductive Carboxylation of Glutamine with Glycolysis in Cells with Mitochondrial Dysfunction. *Mol. Cell* **69**, 581-593.e7 (2018).
 51. Cantó, C. *et al.* AMPK regulates energy expenditure by modulating NAD⁺ metabolism and SIRT1 activity. *Nature* **458**, 1056–1060 (2009).
 52. Bao, X. R. *et al.* Mitochondrial dysfunction remodels one-carbon metabolism in human cells. *eLife* **5**, e10575 (2016).
 53. Kanehisa Laboratories. Kyoto Encyclopedia of Genes and Genomes. Kanehisa Laboratories. KEGG MODULE: 00020. 7 September 2020. World Wide Web URL: <https://www.genome.jp/kegg/>. https://www.kegg.jp/kegg-bin/show_module?hsa_M00020.
 54. Weizmann Institute of Science. Gene Cards: The Human Gene Database. Weizmann

Institute of Science. GCID: GC02P190880. 7 September 2020. World Wide Web URL:
www.genecards.org/. <https://www.genecards.org/cgi-bin/carddisp.pl?gene=GLS>.

55. Chen, Q. *et al.* Rewiring of Glutamine Metabolism Is a Bioenergetic Adaptation of Human Cells with Mitochondrial DNA Mutations. *Cell Metab.* **27**, 1007-1025.e5 (2018).
56. Morvan, D. & Demidem, A. NMR metabolomics of fibroblasts with inherited mitochondrial Complex I mutation reveals treatment-reversible lipid and amino acid metabolism alterations. *Metabolomics* **14**, 55 (2018).
57. Johnson, S. C. *et al.* Regional metabolic signatures in the Ndufs4(KO) mouse brain implicate defective glutamate/ α -ketoglutarate metabolism in mitochondrial disease. *Mol. Genet. Metab.* **130**, 118–132 (2020).
58. Birsoy, K. *et al.* An Essential Role of the Mitochondrial Electron Transport Chain in Cell Proliferation Is to Enable Aspartate Synthesis. *Cell* **162**, 540–551 (2015).
59. Quirós, P. M. *et al.* Multi-omics analysis identifies ATF4 as a key regulator of the mitochondrial stress response in mammals. *J. Cell Biol.* **216**, 2027–2045 (2017).
60. Carelli, V. *et al.* Mitochondria: Biogenesis and mitophagy balance in segregation and clonal expansion of mitochondrial DNA mutations. *Int. J. Biochem. Cell Biol.* **63**, 21–24 (2015).
61. Robitaille, A. M. *et al.* Quantitative Phosphoproteomics Reveal mTORC1 Activates de Novo Pyrimidine Synthesis. *Science* **339**, 1320–1323 (2013).
62. Ben-Sahra, I., Howell, J. J., Asara, J. M. & Manning, B. D. Stimulation of de Novo Pyrimidine Synthesis by Growth Signaling Through mTOR and S6K1. *Science* **339**, 1323–1328 (2013).
63. Ben-Sahra, I., Hoxhaj, G., Ricoult, S. J. H., Asara, J. M. & Manning, B. D. mTORC1 induces purine synthesis through control of the mitochondrial tetrahydrofolate cycle. *Science* **351**, 728–733 (2016).

64. Dibble, C. C. & Manning, B. D. Signal integration by mTORC1 coordinates nutrient input with biosynthetic output. *Nat. Cell Biol.* **15**, 555–564 (2013).
65. Liu, G. Y. & Sabatini, D. M. Author Correction: mTOR at the nexus of nutrition, growth, ageing and disease. *Nat. Rev. Mol. Cell Biol.* **21**, 246–246 (2020).
66. Khan, N. A. *et al.* mTORC1 Regulates Mitochondrial Integrated Stress Response and Mitochondrial Myopathy Progression. *Cell Metab.* **26**, 419–428.e5 (2017).
67. Forsström, S. *et al.* Fibroblast Growth Factor 21 Drives Dynamics of Local and Systemic Stress Responses in Mitochondrial Myopathy with mtDNA Deletions. *Cell Metab.* **30**, 1040–1054.e7 (2019).
68. Dai, Y. *et al.* Rapamycin drives selection against a pathogenic heteroplasmic mitochondrial DNA mutation. *Hum. Mol. Genet.* **23**, 637–647 (2014).
69. Twig, G., Hyde, B. & Shirihai, O. S. Mitochondrial fusion, fission and autophagy as a quality control axis: The bioenergetic view. *Biochim. Biophys. Acta BBA - Bioenerg.* **1777**, 1092–1097 (2008).
70. Chung, C.-Y. *et al.* Maladaptive nutrient signalling sustains the m.3243A>G mtDNA mutation. <http://biorxiv.org/lookup/doi/10.1101/2020.06.18.159103> (2020)
doi:10.1101/2020.06.18.159103.
71. Yu, A. K., Datta, S., McMackin, M. Z. & Cortopassi, G. A. Rescue of cell death and inflammation of a mouse model of complex 1-mediated vision loss by repurposed drug molecules. *Hum. Mol. Genet.* **26**, 4929–4936 (2017).
72. Siegmund, S. E. *et al.* Low-dose rapamycin extends lifespan in a mouse model of mtDNA depletion syndrome. *Hum. Mol. Genet.* **26**, 4588–4605 (2017).
73. Civiletto, G. *et al.* Rapamycin rescues mitochondrial myopathy via coordinated activation of autophagy and lysosomal biogenesis. *EMBO Mol. Med.* **10**, (2018).
74. Barriocanal-Casado, E. *et al.* Rapamycin administration is not a valid therapeutic strategy

- for every case of mitochondrial disease. *EBioMedicine* **42**, 511–523 (2019).
75. Ron, D. Translational control in the endoplasmic reticulum stress response. *J. Clin. Invest.* **110**, 1383–1388 (2002).
 76. Harding, H. P. *et al.* An Integrated Stress Response Regulates Amino Acid Metabolism and Resistance to Oxidative Stress. *Mol. Cell* **11**, 619–633 (2003).
 77. Krishnamoorthy, T., Pavitt, G. D., Zhang, F., Dever, T. E. & Hinnebusch, A. G. Tight Binding of the Phosphorylated α Subunit of Initiation Factor 2 (eIF2 α) to the Regulatory Subunits of Guanine Nucleotide Exchange Factor eIF2B Is Required for Inhibition of Translation Initiation. *Mol. Cell. Biol.* **21**, 5018–5030 (2001).
 78. Pakos-Zebrucka, K. *et al.* The integrated stress response. *EMBO Rep.* **17**, 1374–1395 (2016).
 79. Rutkowski, D. T. *et al.* Adaptation to ER Stress Is Mediated by Differential Stabilities of Pro-Survival and Pro-Apoptotic mRNAs and Proteins. *PLoS Biol.* **4**, e374 (2006).
 80. Jazwinski, S. M. The retrograde response: When mitochondrial quality control is not enough. *Biochim. Biophys. Acta BBA - Mol. Cell Res.* **1833**, 400–409 (2013).
 81. Cortopassi, G. *et al.* Mitochondrial disease activates transcripts of the unfolded protein response and cell cycle and inhibits vesicular secretion and oligodendrocyte-specific transcripts. *Mitochondrion* **6**, 161–175 (2006).
 82. Weizmann Institute of Science. Gene Cards: The Human Gene Database. Weizmann Institute of Science. GCID: GC22P039525. 7 September 2020. World Wide Web URL: www.genecards.org/. <https://www.genecards.org/cgi-bin/carddisp.pl?gene=ATF4>.
 83. Ameri, K. & Harris, A. L. Activating transcription factor 4. *Int. J. Biochem. Cell Biol.* **40**, 14–21 (2008).
 84. Chen, H., Pan, Y.-X., Dudenhausen, E. E. & Kilberg, M. S. Amino Acid Deprivation Induces the Transcription Rate of the Human Asparagine Synthetase Gene through a

- Timed Program of Expression and Promoter Binding of Nutrient-responsive Basic Region/Leucine Zipper Transcription Factors as Well as Localized Histone Acetylation. *J. Biol. Chem.* **279**, 50829–50839 (2004).
85. Ameri, K. *et al.* Anoxic induction of ATF-4 through HIF-1-independent pathways of protein stabilization in human cancer cells. *Blood* **103**, 1876–1882 (2004).
 86. Melber, A. & Haynes, C. M. UPRmt regulation and output: a stress response mediated by mitochondrial-nuclear communication. *Cell Res.* **28**, 281–295 (2018).
 87. Fujita, Y. *et al.* CHOP (C/EBP homologous protein) and ASNS (asparagine synthetase) induction in cybrid cells harboring MELAS and NARP mitochondrial DNA mutations. *Mitochondrion* **7**, 80–88 (2007).
 88. Kim, K. H. *et al.* Metformin-induced inhibition of the mitochondrial respiratory chain increases FGF21 expression via ATF4 activation. *Biochem. Biophys. Res. Commun.* **440**, 76–81 (2013).
 89. Tyynismaa, H. *et al.* Mitochondrial myopathy induces a starvation-like response. *Hum. Mol. Genet.* **19**, 3948–3958 (2010).
 90. Bouman, L. *et al.* Parkin is transcriptionally regulated by ATF4: evidence for an interconnection between mitochondrial stress and ER stress. *Cell Death Differ.* **18**, 769–782 (2011).
 91. Emperador, S. *et al.* Ketogenic treatment reduces the percentage of a LHON heteroplasmic mutation and increases mtDNA amount of a LHON homoplasmic mutation. *Orphanet J. Rare Dis.* **14**, 150 (2019).
 92. Bustin, S. A. *et al.* The MIQE Guidelines: Minimum Information for Publication of Quantitative Real-Time PCR Experiments. *Clin. Chem.* **55**, 611–622 (2009).
 93. Johnson, S. C. *et al.* mTOR Inhibition Alleviates Mitochondrial Disease in a Mouse Model of Leigh Syndrome. *Science* **342**, 1524–1528 (2013).

94. Park, Y., Reyna-Neyra, A., Philippe, L. & Thoreen, C. C. mTORC1 Balances Cellular Amino Acid Supply with Demand for Protein Synthesis through Post-transcriptional Control of ATF4. *Cell Rep.* **19**, 1083–1090 (2017).
95. Han, J. *et al.* ER-stress-induced transcriptional regulation increases protein synthesis leading to cell death. *Nat. Cell Biol.* **15**, 481–490 (2013).
96. Kaufman, R. J. *et al.* The unfolded protein response in nutrient sensing and differentiation. *Nat. Rev. Mol. Cell Biol.* **3**, 411–421 (2002).
97. Brown, M. D., Trounce, I. A., Jun, A. S., Allen, J. C. & Wallace, D. C. Functional Analysis of Lymphoblast and Cybrid Mitochondria Containing the 3460, 11778, or 14484 Leber's Hereditary Optic Neuropathy Mitochondrial DNA Mutation. *J. Biol. Chem.* **275**, 39831–39836 (2000).

Acknowledgements

This work has been funded by the Program Talento Modalidad 1 from the Comunidad de Madrid conceded to Dr. Aurora Gómez-Durán (2019-T1/BMD-14236).

I would like to thank the Universidad Francisco de Vitoria and the Centro de Investigaciones Biológicas 'Margarita Salas' for giving me this opportunity. Especial thanks to Dr. Aurora Gómez-Durán for letting me work in her project, for her persevering tutoring and help along this work. Thanks to Dr. Teresa de Asua for her tutoring. Special thanks to my family and friends for their loving support.